animals

MDPI

Article

Maternal effects and trophodynamics drive interannual larval growth variability of Atlantic bluefin tuna (*Thunnus thynnus*) from the Gulf of Mexico.

José Mª Quintanilla [a,*], Ricardo Borrego-Santos [a,b], Estrella Malca [c,d], Rasmus Swalethorp [e], Michael R. Landry [e], Trika Gerard [d], John Lamkin [d], Alberto García [a] and Raúl Laiz Carrión [a].

[a] Instituto Español de Oceanografía (IEO-CSIC), Centro Oceanográfico de Málaga, Fuengirola, Spain
[b] Departamento de Biología Animal, Facultad de Ciencias, Universidad de Málaga, Málaga, Spain
[c] Cooperative Institute for Marine and Atmospheric Studies, University of Miami, Miami, FL, USA
[d] NOAA Fisheries, Southeast Fisheries Science Center, Miami, FL, USA
[e] Scripps Institution of Oceanography, University of California San Diego, La Jolla, CA, USA
* Correspondence: jose.quintanilla@ieo.csic.es.

Simple Summary: Environmental factors, maternal inheritance, and feeding success are influential factors in fish growth, especially during the larval stage, encompassing their early days of life. Growth rates play a crucial role in larval survival, particularly in species with high energy requirements such as the Atlantic bluefin tuna (ABFT). Our analyses of two patches of ABFT larvae collected in the Gulf of Mexico spawning region during different years reveal variable larval growth, depending on prey availability. Larval growth also shows a direct relationship to maternal feeding. Estimates of larval trophic positions are primarily influenced by food web length and energy transmission efficiency, leading to differences in larval growth and underscoring the importance of considering trophic dynamics in results interpretation. These findings offer novel insights into how these factors affect ABFT larval growth, potentially informing conservation efforts and fisheries management strategies by governmental institutions.

Abstract: Two populations of Atlantic bluefin tuna (*Thunnus thynnus*) larvae were collected in 2017 and 2018 during the peak of spawning in the Gulf of Mexico (GOM). We examined environmental variables, daily growth, otolith biometry and stable isotopes and found that GOM18 larval cohorts grew at faster rates, with larger and wider otoliths. Inter and intra-population analyses (deficient vs. optimal growth groups) for pre- and post-flexion developmental stages were done to determine maternal and trophodynamic influences on larval growth variability based on larval isotopic signatures, trophic niche sizes and their overlaps. For pre-flexion stages in both years, optimal growth groups had significantly lower $\delta^{15}N$ implying a direct relationship between growth potential and maternal inheritance. Optimal growth groups and stages for both years showed lower C:N ratios reflecting a greater energy investment in growth. The result of this study reflect the interannual transgenerational trophic plasticity of a spawning stock and its linkages to the growth potential of their offspring within GOM.

Keywords: Atlantic bluefin tuna - Larval growth - Trophic ecology - Isotopic signatures - Maternal effects - Trophic niches

Citation: José Mª Quintanilla a,*; Borrego-Santos a, R.; Malca c, E.; Swalethorp e, R.; Landry e, M.R.; Gerard d, T.; Lamkin d, J.; García a, A.; Carrión a, R.L. Maternal effects and trophodynamics drive interannual larval growth variability of Atlantic bluefin tuna (*Thunnus thynnus*) from the Gulf of Mexico. *Animals* **2024**, *14*, x. https://doi.org/10.3390/xxxxx

Academic Editor(s): Name

Received: date
Revised: date
Accepted: date
Published: date

Introduction

Top predatory fishes in mid- to high latitude marine ecosystems play crucial roles in the stability of food web structure [1,2]. For Atlantic Bluefin Tuna (ABFT, *Thunnus thynnus*), cascading effects of population fluctuations can alter the structure and performance of the lower food web [3-5].

ABFT is managed by the International Commission for the Conservation of Atlantic tunas (ICCAT) as two, eastern and western, stocks [6] with different natal homing behaviors, spawning areas, sexual maturity ages, and trophic dynamics [7-9]. The western stock feeds principally in prey-rich waters of the north and northwestern Atlantic [11-14]. Displaying a capital feeding strategy for reproduction [15,16] nutritionally replenished adults migrate thousands of kilometers each year to reproduce in the warm oligotrophic waters of the Gulf of Mexico (GOM) [17,10].

The continental shelf of the GOM is a very productive area due in part to the supply of fresh water and nutrients from numerous rivers, principally the Mississippi River [18-23] which transport nutrients hundreds of kilometers [23] to strongly oligotrophic oceanic waters of the GOM [24-26]. These oligotrophic spawning grounds for ABFT [17] have strong hydrographic features driven by the Loop Current [27]. This current enters the GOM just east of the Yucatan Peninsula, loops along in a circular path and exits towards the southeast through the Florida Strait [28]. The shape of the current is influenced by the bathymetry of the Yucatan Peninsula, that propitiates the formation of westward-moving eddies, gyres and frontal structures and establishes the characteristic mesoscale hydrographical circulation within the GOM basin [29]. It is the mesoscale features that are ideal ABFT larval nursery habitats [30]. Spawning occurs from April to June [31] and is triggered by the increase of temperature of surface waters (above 24ºC) [17].

The two main environmental influences on the early life stages of tunas are temperature and food availability [32-36]. Temperature influences vital and metabolic rates that in turn affect rates of growth and mortality [37,38]. Temperature enhances growth rate of tuna larvae if food availably is sufficient [32,39,34] and is the main abiotic driver of tuna distribution and recruitment [40].

Successful and frequent feeding during early life history depends on adequate food resources and is essential for survival. Knowledge of the relationship between growth and trophic ecology is fundamental for understanding how larvae respond to varying spatio-temporal dynamics of their nursery habitat [41,42]. Environmental impacts on the stock-recruitment relationship for ABFT result in varying recruitment scenarios and informs management decisions on fishing pressure and stock recovery potential. Understanding larval survival rates and the stock-recruitment relationship in their spawning grounds is critical for effective management.

Trophic studies in fish larvae have mostly focused on stomach content analyses which give snapshots of prey consumed over relatively short feeding periods [43-46]. Stable isotope analyses (SIA) complement traditional gut content examination with biogeochemical information on the mean trophic characteristics of prey consumed over a longer time scale, essentially the nutritional history of the larvae up to the point of capture [47,15,48].

Nitrogen ($\delta^{15}N$) and carbon ($\delta^{13}C$) SIA are often used to assess trophic position and carbon flows to consumers in food webs [49-51]. Nitrogen $\delta^{15}N$ is an indicator of the mean N sources supporting consumer growth and enriches with each trophic transfer in the food chain. Since C isotope ratios undergo small changes during trophic transfers, $\delta^{13}C$ is mainly used to assess how food sources with different mean $\delta^{13}C$ values contribute to diet [50, 52]. SIA has been previously applied to evaluate trophic influences on larval growth of ABFT using size-fractionated zooplankton as baseline values [53].

Isotopic signatures ($\delta^{15}N$ and $\delta^{13}C$) evolve as different prey types are selected by larval of increasing size and developmental stage [54,55]. For pre-flexion stages, $\delta^{15}N$ signatures are derived principally from maternal transmission [56], corresponding to the consumer isotopic signatures of adult breeding females. In contrast, $\delta^{15}N$ for post-flexion stages, increases with size and development and reflects larval dietary changes [54]. In field samples, this trophic change is interpreted as a tendency towards larger prey-size consumption with age [55,57]. These larval $\delta^{15}N$ values, together with the baseline isotopic signature of the microzooplankton community (0.05 - 0.2 mm in size), allow us to estimate and compare TPs among populations and to understand the ecological roles of different

species in the system [51, 58], their trophic structure and consumer-prey relationships [59]. Therefore, TP estimation is crucial for understanding trophodynamics and the influence of trophic interactions on larval growth variability.

Stable isotopes are also used to estimate trophic parameters, such as maternal/trophic isotopic niche widths and niche overlap, by applying stable isotope Bayesian inference [60]. These niches are measures of dietary diversity [61-63] and describe the isotopic characteristics of the niches exploited by the breeders (maternal) and larvae (trophic) of the species.

In this study, growth variability of two ABFT larval cohorts (2017 and 2018) are compared from two complementary perspectives: inter and intra-population analysis. We analyzed larval daily growth with trophodynamics characterized by SIA analysis and isotopic niches considering both the total population (TOTAL) and the segregated groups of pre-flexion (PRE) and post-flexion (POST) larvae, which respectively reflect maternal and larval trophodynamic influences.

Materials and Methods

Sampling and processing of ABFT larvae and plankton

Samples of ABFT larvae and zooplankton prey were collected in the Gulf of Mexico spawning region at 9 stations on BLOOFINZ cruise NF1704 (May 2017) and at 19 stations on BLOOFINZ cruise NF1802 (May 2018) aboard NOAA R/V Nancy Foster (Figure 1). On each cruise, we first located a patch of significant larval abundance with preliminary net tows, then marked the patch with a free-floating satellite-tracked drifter with a 3-m drogue centered at 15-m in the surface mixed layer and repeatedly sampled the larvae and ambient zooplankton prey in the same water over the course of 3-4 days [64]. Larval patches GOM17 and GOM18 in Figure 1 were found at different locations, GOM18 being closer to the richer continental margin than GOM17, which was well into oligotrophic waters of the central GOM. However, both larval patches were found to have originated ~2-4 weeks earlier at roughly the same location along the northwest continental margin of the GOM by backtracking drift trajectories in a reanalysis of surface water circulation [64]. This study therefore compares two groups of ABFT larvae originating from the same general location in different years but experiencing different trophic conditions.

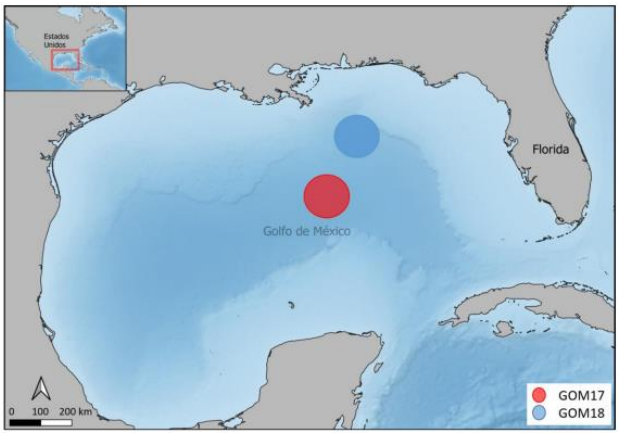

Figure 1. - Area of larval ABFT tuna sampling stations during the BLOOFINZ surveys 2017 and 2018.

For ABFT larvae, we used a Bongo 90 cm net frame with 500 μm mesh towed obliquely from the surface to 25 m and back at approximately 2 knots for 10 minutes. Zooplankton samples were collected on the same tows as the larvae, using a 20-cm Bongo net frame with 200 and 55 μm mesh nets attached to the Bongo 90 cm net frame [53]. Each of the Bongo 90 and Bongo 20 nets was equipped with a General Oceanics flowmeter to measure the volume of water filtered during each tow (m^3). Temperature (°C) and salinity

(psu) profiles for the upper 25 m were determined from CTD casts conducted concurrently at each station (see [65] for hydrographic sampling details).

ABFT larvae were sorted, preserved and processed on board following [66] to obtain standard length (SL, mm) and dry weights (DW, mg). Specimens were freeze-dried and placed in individual tin capsules (0.2 - 2 mg) for SIA analyses

Zooplankton from each net were spilt in two subsamples and preserved following [46]: from the 55 μm mesh, one subsample was frozen at -20°C for biomass and SIA, and the other preserved with 4% formaldehyde for community analysis. The two subsamples from the 200 μm mesh net were concentrated and frozen at -20°C and preserved in ethanol 96%, respectively.

Otolith analyses

Otoliths were removed, cleaned with distilled water and fixed on slides with one drop of nail lacquer [66]. Sagittal otoliths were digitalized as stacks of focal-depth images, varying in number depending on otolith size. Otoliths were excluded if they were broken, not saggitae or had fixation artifacts. Otolith radius (RADIUS, μm), daily increments (AGE, days) and mean increment widths (MIW, μm), were also measured by Leica image analysis software. Reading criteria for ABFT larval age estimations were previously applied [35,66,67] and detailed by Malca et al. [65].

SIA analyses of larvae and zooplankton

Natural abundance of N ($\delta^{15}N$) and C ($\delta^{13}C$) were measured with an isotope-ratio spectrometer (Thermo-Finningan Deltaplus) coupled to an elemental analyzer (FlashEA1112 Thermo-Finningan) at the Instrumental Unit of Analysis of the University of A Coruña. Ratios of ^{15}N:^{14}N and ^{12}C:^{13}C are expressed in conventional delta notation (δ), relative to the international standard [atmospheric air (N_2) and Pee-Dee Belemnite (PDB), respectively, using acetanilide as standard]. The analytical precision for $\delta^{15}N$ and $\delta^{13}C$ were 0.13 and 0.11‰, respectively, based on the standard deviation of internal references (repeatability of duplicates) A posteriori corrections of $\delta^{13}C$ values for lipid content were done based on C:N ratios for micro- and mesozooplankton size fractions according to the equations and parameters for invertebrates [68] and for muscle tissue of ABFT larvae [53].

Estimation of isotopic maternal signatures

We estimated isotopic maternal values using the model of Uriarte et al. [54]:

$$\delta^{15}N_{MATERNAL} = \delta^{15}N_{LARVAE} + (\delta^{15}N_{EGG} - \delta^{15}N_{LARVAE})$$

$$\delta^{13}C_{MATERNAL} = \delta^{13}C_{LARVAE} + (\delta^{13}C_{EGG} - \delta^{13}C_{LARVAE})$$

where $\delta^{15}N_{larvae}$ and $\delta^{13}C_{larvae}$ are bulk SIA values for each larva. To calculate the factors ($\delta^{15}N_{egg}$ - $\delta^{15}N_{larva}$) and ($\delta^{13}C_{egg}$ - $\delta^{13}C_{larva}$) required for estimating maternal isotopic values, we used the isotopic values for each pre-flexion larva on each survey to determine a linear relationship of isotope variability with age (Table 1).

Table 1. - Maternal isotopic signature equations derived from larvae captured in the field (GOM17 and GOM18). NS= Non-significant; * $p < 0.05$; ** $p < 0.01$. .

Population	N	Maternal isotopic signature estimation equation	*p*	R^2
GOM17	49	$(\delta^{15}N_{EGG} - \delta^{15}N_{LARVAE}) = (7.206 + 0.047 * AGE)$	NS	0.01
		$(\delta^{13}C_{EGG} - \delta^{13}C_{LARVAE}) = (0.467 + 0.091 * AGE)$	*	0.09
GOM18	52	$(\delta^{15}N_{EGG} - \delta^{15}N_{LARVAE}) = (0.975 + 0.527 * AGE)$	**	0.52
		$(\delta^{13}C_{EGG} - \delta^{13}C_{LARVAE}) = (2.423 - 0.200 * AGE)$	**	0.45

The $\delta^{15}N$ and $\delta^{13}C$ values for eggs were obtained from newly spawned eggs and lecithotrophic larvae (n = 20 pooled) from the aquaculture rearing experiments [54]. For wild ABFT larvae, the isotopic values of eggs were calculated using a random variable originating from the mean and standard deviation of egg and lecithotrophic larvae of the rearing experiment [66].

Larval trophic positions

The trophic position (TP) of each ABFT larvae was calculated following Eq (1):

$$TP = \frac{\delta^{15}N_{LARVAE} - \delta^{15}N_{MICRO}}{\Delta^{15}N} + TP_{BASAL}$$

where $\delta^{15}N_{LARVAE}$ is the larval N isotopic signatures and $\delta^{15}N_{MICRO}$ is the isotopic value for microzooplankton at the same station. We applied a basal trophic position (TP_{BASAL}) of 2, assuming microzooplankton as primary consumers [69]. For Nitrogen isotopic discrimination factor ($\Delta^{15}N$), we used the muscle tissue value for juveniles ABFT (1.46 ‰) proposed by [70] and previously applied to ABFT larvae by [65].

Maternal and larval isotopic niche widths and overlaps

Maternal isotopic niches widths were estimated from $\delta^{15}N_{maternal}$ and $\delta^{13}C_{maternal}$ values, calculated from the isotopic values of pre-flexion larvae. Larval isotopic niches widths were calculated from $\delta^{15}N$ and $\delta^{13}C$ values of post-flexion specimens' stages in order to avoid the maternal influence. The isotopic niche widths were estimated by standard Bayesian ellipse areas and associated credible interval adjusted for small sample size (SEAc) [60, 68]. Isotopic niche widths and overlap analyses were conducted using the R package SIBER (Stable Isotope Bayesian Ellipses in R) v.3.3.0 ([60], R Development Core Team 2012). Standard ellipses were calculated from the variance and covariance of 40% of the bivariate data.

Statistical analyses

Environmental variables were compared with non-parametric Mann-Whitney U test as the variables did not meet parametric assumptions. Significance tests for differences growth, isotopic signatures, C:N values and otolith metrics between GOM17 and GOM18 larval groups were done by ANCOVA using AGE as the covariable. The variables were Log transformed prior to statistical analyses when necessary to obtain linearity and variance homogeneity [71]. When there was no linear relationship of a variable with AGE, an ANOVA analysis was used to determine differences between groups.

We used linear equations (y=a+x*b) for LogSL and LogDW vs AGE to define the daily growth pattern of each larval population, and their residual values were obtained with respect the whole population. GOM17 and GOM18 populations were divided into four groups according to their residual values of length (SL) and weight (DW) controlled by AGE. Larger and heavier than expected larvae were in the OPT group, with positive residuals for both fits, while smaller and lighter than expected larvae were in the DEF group, with negative residuals for both fits. Two intermediate groups (shorter SL but heavier and vice versa) were not considered in this study. Following the method of [72], the residual analysis defined groups according to optimal (OPT) and deficient (DEF) growth patterns in length (SL) and weight (DW) of individual larvae. For intra-population comparisons, these groups were compared through an ANCOVA analysis controlled by AGE [66].–

For isotopic niche widths, the color scale (dark, medium and light) represents confidence intervals of 50%, 75% and 95% respectively. Isotopic niche widths and overlap

analyses were conducted using the R package SIBER (Stable Isotope Bayesian Ellipses in R) v.3.3.0 (Jackson et al. 2011, R Development Core Team 2012).

Statistical analyses were done using R version 4.2.1 (R Core Team 23-6-22 ucrt) through the integrated development environment RStudio, with $\alpha = 0.05$.

Results

Environmental and abiotic variables

Environmental variables showed significant differences between years with higher temperatures and lower salinities for GOM18. The isotopic signatures of micro and mesozooplankton fractions were higher in $\delta^{15}N$ and lower in $\delta^{13}C$ for GOM18 (Table 2).

Table 2. - Mean values (Mean ± SD) of temperature (TEMP, °C), salinity (SAL, ppt), $\delta^{15}N$ and $\delta^{13}C$ of microzooplankton and mesozooplankton. U Mann Whitney Test. ** $p < 0.01$. .

	GOM17	GOM18	MW - U test	
	MEAN ± SD	**MEAN ± SD**	***Z-adjusted***	***p***
TEMP (C°)	24.69 ± 0.67	25.53 ± 0.47	-2.72	**
SAL (ppt)	36.38 ± 0.06	36.02 ± 0.32	3.30	**
$\delta^{15}N_{MICRO}$	0.56 ± 0.42	3.61 ± 0.39	-3.00	**
$\delta^{13}C_{MICRO}$	-18.1 ± 0.47	-19.3 ± 0.27	3.00	**
$\delta^{15}N_{MESO}$	1.75 ± 0.51	4.69 ± 0.42	-2.74	**
$\delta^{13}C_{MESO}$	-17.7 ± 0.52	-19.6 ± 0.25	2.74	**

Larval growth

Larval growth showed a normal distribution with a common size range (4-9 mm) for both groups (Figure A1). For the TOTAL group, somatic and otolith biometrics differed between years, with higher values of SL, DW, RADIUS and MIW in GOM18 (Figure A2 and Table 3).

Table 3. - Larval somatic data (SL, DW) and biometric otoliths (RADIUS, MIW) for GOM17 and GOM18 grouped by stage (PRE, POST, TOTAL). ANCOVA results (F, p) using AGE as covariate. NS= Non-significant; * $p < 0.05$; ** $p < 0.01$.

		GOM17				GOM18				ANCOVA	
		N	**MIN**	**MAX**	**MEAN ± SD**	**N**	**MIN**	**MAX**	**MEAN ± SD**	**$F_{1,154}$**	***p***
TOTAL	SL (mm)	83	4.28	9.01	6.04 ± 1.10	74	4.1	9.87	6.23 ± 1.43	5.42	*
	DW (mg)		0.1	2.89	0.49 ± 0.45		0.07	2.51	0.70 ± 0.61	26.78	**
	RADIUS (µm)		16.7	95.4	30.5 ± 13.50		13.8	89.3	33.00 ± 18.40	3.24	NS
	MIW ((µm)		1.28	4.15	2.03 ± 0.60		1.06	4.64	2.16 ± 0.83	6.01	*
		N	**MIN**	**MAX**	**MEAN ± SD**	**N**	**MIN**	**MAX**	**MEAN ± SD**	**$F_{1,82}$**	***p***
PRE	SL (mm)	49	4.28	7.06	5.34 ± 0.68	36	4.1	6.36	5.06 ± 0.57	0.04	NS
	DW (mg)		0.1	0.52	0.27 ± 0.12		0.07	0.64	0.30 ± 0.14	6.33	*
	RADIUS (µm)		16.7	33.4	23.26 ± 4.08		13.8	28	20.10 ± 3.61	5.66	*
	MIW ((µm)		1.28	2.22	1.70 ± 0.25		1.06	2.06	1.53 ± 0.27	3.87	NS
		N	**MIN**	**MAX**	**MEAN ± SD**	**N**	**MIN**	**MAX**	**MEAN ± SD**	**$F_{1,69}$**	***p***
POST	SL (mm)	34	6.08	9.01	7.04 ± 0.75	38	5.83	9.87	7.39 ± 1.01	11.02	**
	DW (mg)		0.21	2.89	0.81 ± 0.56		0.37	2.51	1.08 ± 0.63	20.9	**
	RADIUS (µm)		27.4	95.4	40.93 ± 15.36		23.5	89.3	44.85 ± 18.38	7.91	**
	MIW ((µm)		1.78	4.15	2.51 ± 0.63		1.76	4.64	2.77 ± 0.73	6.52	**

For pre-flexion larvae, SL did not differ between years, while GOM18 had higher DW and GOM17 had larger RADIUS and MIW (Figure A3 and Table 3). In contrast, somatic

and otolith variables were both consistently higher in GOM18 for post-flexion (Figure. A4 and Table 3). At the intra-population level, every growth pattern differed for both development stages, showing higher mean values for OPT larvae (Figures A3 and A4 and Table 4).

Table 4. - Larval somatic data (SL, DW) and biometric otoliths (RADIUS, MIW) of each year (GOM17, GOM18) grouping by stage (PRE, POST, TOTAL). ANCOVA analysis result (F, p) using AGE as covariate.** $p < 0.01$.

			OPT(+)				DEF(-)				ANCOVA		ANOVA	
			N	MIN	MAX	MEDIA ± SD	N	MIN	MAX	MEDIA ± SD	$F_{1,52}$	*p*		
TOTAL	GOM17	SL (mm)	27	5.4	8.71	6.78 ± 0.78	28	4.3	9.01	5.52 ± 1.05	115.3	***		
		DW (mg)		0.3	2.13	0.69 ± 0.38		0.1	2.89	0.36 ± 0.54	140.8	***		
		RADIUS (µm)		23	79.3	36.30 ± 12.20		17.3	95.4	26.90 ± 15.20	63.98	***		
		MIW ((µm)		1.8	4.14	2.41 ± 0.57		1.28	4.01	1.73 ± 0.54	34.14	***		
			N	MIN	MAX	MEDIA ± SD	N	MIN	MAX	MEDIA ± SD	$F_{1,59}$	*p*		
	GOM18	SL (mm)	36	4.8	8.98	6.86 ± 1.03	26	4.1	9.87	5.77 ± 1.77	180.8	***		
		DW (mg)		0.29	2.42	0.85 ± 0.43		0.09	2.51	0.64 ± 0.83	132.4	***		
		RADIUS (µm)		15	77.5	36.90 ± 13.50		15.8	89.3	32.00 ± 25.20	79.73	***		
		MIW ((µm)		1.3	4.64	2.51 ± 0.69		1.06	4.22	1.89 ± 0.96	40.56	***		
			N	MIN	MAX	MEDIA ± SD	N	MIN	MAX	MEDIA ± SD	$F_{1,27}$	*p*		
PRE	GOM17	SL (mm)	15	4.3	7.06	5.79 ± 0.78	15	4.3	5.6	5.05 ± 0.36	55.85	**		
		DW (mg)		0.2	0.52	0.37 ± 0.11		0.1	0.25	0.18 ± 0.05	77.96	**		
		RADIUS (µm)		17	33.4	25.70 ± 4.25		17.9	26.8	21.78 ± 2.59	29.5	**		
		MIW ((µm)		1.52	2.22	1.91 ± 0.18		1.28	1.83	1.53 ± 0.17	37.62	**		
			N	MIN	MAX	MEDIA ± SD	N	MIN	MAX	MEDIA ± SD	$F_{1,23}$	*p*	$F_{1,23}$	*p*
	GOM18	SL (mm)	11	4.8	6.2	5.59 ± 0.42	14	4.1	5.04	4.66 ± 0.27	152.18	**	34.08	**
		DW (mg)		0.3	0.64	0.44 ± 0.12		0.09	0.38	0.20 ± 0.08				
		RADIUS (µm)		15	26.4	22.74 ± 3.32		15.8	22.4	18.29 ± 2.29	54.73	**		
		MIW ((µm)		1.26	2.06	1.79 ± 0.22		1.06	1.64	1.32 ± 0.17	51.11	**		
			N	MIN	MAX	MEDIA ± SD	N	MIN	MAX	MEDIA ± SD	$F_{1,26}$	*p*		
POST	GOM17	SL (mm)	14	6.6	8.71	7.42 ± 0.68	11	6.08	9.01	6.78 ± 0.87	45.46	**		
		DW (mg)		0.5	2.13	0.97 ± 0.50		0.21	2.89	0.70 ± 0.77	45.38	**		
		RADIUS (µm)		30	79.3	45.90 ± 15.50		27.4	95.4	39.10 ± 19.50	41.71	**		
		MIW ((µm)		2	4.14	2.84 ± 0.70		1.78	4.01	2.24 ± 0.63	26.98	**		
			N	MIN	MAX	MEDIA ± SD	N	MIN	MAX	MEDIA ± SD	$F_{1,26}$	*p*		
	GOM18	SL (mm)	15	6.4	9.19	7.77 ± 0.79	14	5.83	9.25	6.87 ± 1.12	105.9	***		
		DW (mg)		0.5	2.51	1.22 ± 0.59		0.37	2.5	0.86 ± 0.71	56.48	***		
		RADIUS (µm)		28	85.5	49.10 ± 15.90		23.4	89.3	39.80 ± 22.20	57.97	***		
		MIW ((µm)		2.2	4.64	3.16 ± 0.65		1.76	4.07	2.35 ± 0.73	39.15	***		

Larval trophic variables

The inter-population $\delta^{15}N$ and $\delta^{13}C$ values were higher for GOM18 for both pre- and post-flexion stages and TOTAL larvae (Figure 2 and Table A1). Despite GOM18 larvae having higher $\delta^{15}N$ (6.60 ± 0.78 vs. 4.47 ± 0.60), TP values were higher for GOM17 (4.12 ± 0.25 vs. 3.47 ± 0.22) (Figure 2 and Table A1). At the intra-population level for both GOM17 and GOM18, DEF larvae had higher levels of $\delta^{15}N$ and C:N, while $\delta^{13}C$ levels were higher for OPT (Figure 2 and Table A2). We found no intra-population TP differences for either year (Figure 2 and Table A2).

For GOM17 pre-flexion larvae, the DEF group had higher values of $\delta^{15}N$, $\delta^{13}C$ and C:N than OPT. Values of $\delta^{15}N$ were also higher for the DEF group in GOM18, but $\delta^{13}C$ and C:N were not significantly different (Figure 2 and Table A2).

For GOM17 post-flexion larvae, C:N was higher for DEF, but no significant differences were found for $\delta^{15}N$, $\delta^{13}C$ or TP. For GOM18 post-flexion larvae, $\delta^{13}C$ and C:N were higher for the DEF group while $\delta^{15}N$ and TP did not differ between DEF and OPT (Figure 2 and Table A2).

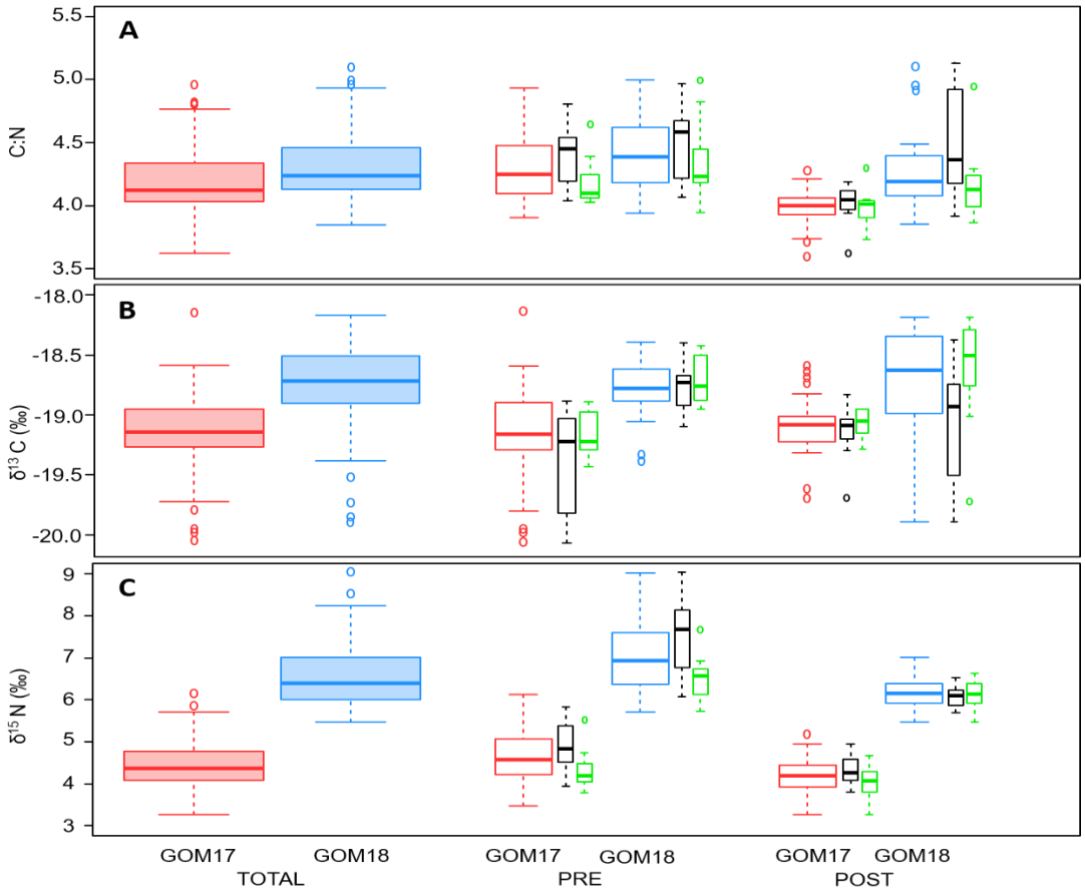

Figure 2. - Boxplot of (A) C:N, (B) $\delta^{13}C$ and (C) $\delta^{15}N$ values of inter (GOM17 – red, GOM18 - blue) and intra-populations (OPT- green, DEF - black).

Trophic Niches

Maternal Trophic Niches

For inter-population comparisons, maternal isotopic signatures showed ellipse area overlaps of 60% (0.49) (Figure 3A) and no significant differences in $\delta^{15}N$ and $\delta^{13}C$ values between years (Table 5), The estimated niche area for GOM17 was slightly larger (0.67) than GOM18 (0.65) (Figure 3B).

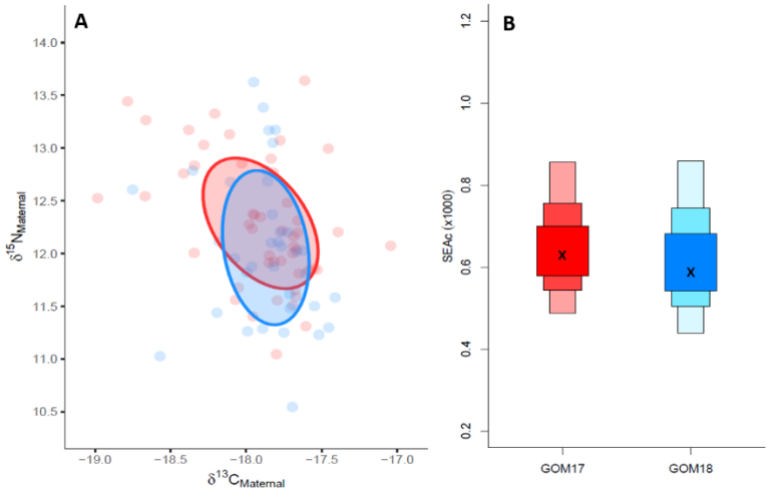

Figure 3. - (A) $\delta^{15}N$ vs $\delta^{13}C$ maternal values for GOM17 and GOM18. Maternal trophic niches are represented by the ellipse areas. (B) Estimated ellipse areas applying the correction for small sample sizes (SEAc).

Table 5. - Inter-population results of Mann-Whitney U test (mean ± SE, number of larvae, Z adjusted and p) between years (GOM17 and GOM18) for maternal isotopic signatures ($\delta^{15}N$maternal, $\delta^{13}C$maternal). NS= Non-significant.

	GOM17		GOM18		MW - U test	
	N	MEAN ± SD	N	MEAN ± SD	*Z-adjusted*	*p*
$\delta^{15}N_{MATERNAL}$ (estimated)	49	12.30 ± 0.61	36	12.10 ± 0.72	1.66	NS
$\delta^{13}C_{MATERNAL}$ (estimated)	49	-17.90 ± 0.38	36	-17.90 ± 0.28	0.07	NS

Table 6. - Intra-population (OPT vs DEF) results of Mann-Whitney U test (mean ± SE, number of larvae, Z adjusted and p) between surveys (GOM17 and GOM18) for maternal isotopic signatures ($\delta^{15}N$maternal, $\delta^{13}C$maternal) estimated by equations based on samples of each survey samples. NS= Non-significant ** p<0.01.

	GOM17						GOM18					
	OPT +		DEF –		MW - U test		OPT +		DEF –		MW - U test	
	MEAN ± SD	N	MEAN ± SD	N	*Z-adjusted*	*p*	MEAN ± SD	N	MEAN ± SD	N	*Z-adjusted*	*p*
$\delta^{15}N_{MATERNAL}$ (estimated)	11.90 ± 0.44	15	12.50 ± 0.61	15	2.76	**	11.50 ± 0.33	11	12.60 ± 0.67	14	3.5	**
$\delta^{13}C_{MATERNAL}$ (estimated)	-17.80 ± 0.22	15	-18.10 ± 0.46	15	-1.68	NS	-17.80 ± 0.35	11	-17.90 ± 0.17	14	-0.6	NS

Comparing optimal growth (OPT) and deficient (DEF) groups, estimated maternal values of $\delta^{15}N$ were significantly different between years, with higher values in the DEF groups. However, estimated maternal $\delta^{13}C$ were not significantly different between OPT and DEF for both years (Table 6).

For GOM2017, maternal niches of the contrasting growth groups overlapped 14% (0.15) (Figure 4A), being larger for DEF (0.89) than OPT (0.31) (Figure 4B). For GOM18, OPT and DEF larvae showed maternal niches of similar sizes (0.38 OPT vs 0.36 DEF) (Figure 4A) with no overlap between them (Figure 4B).

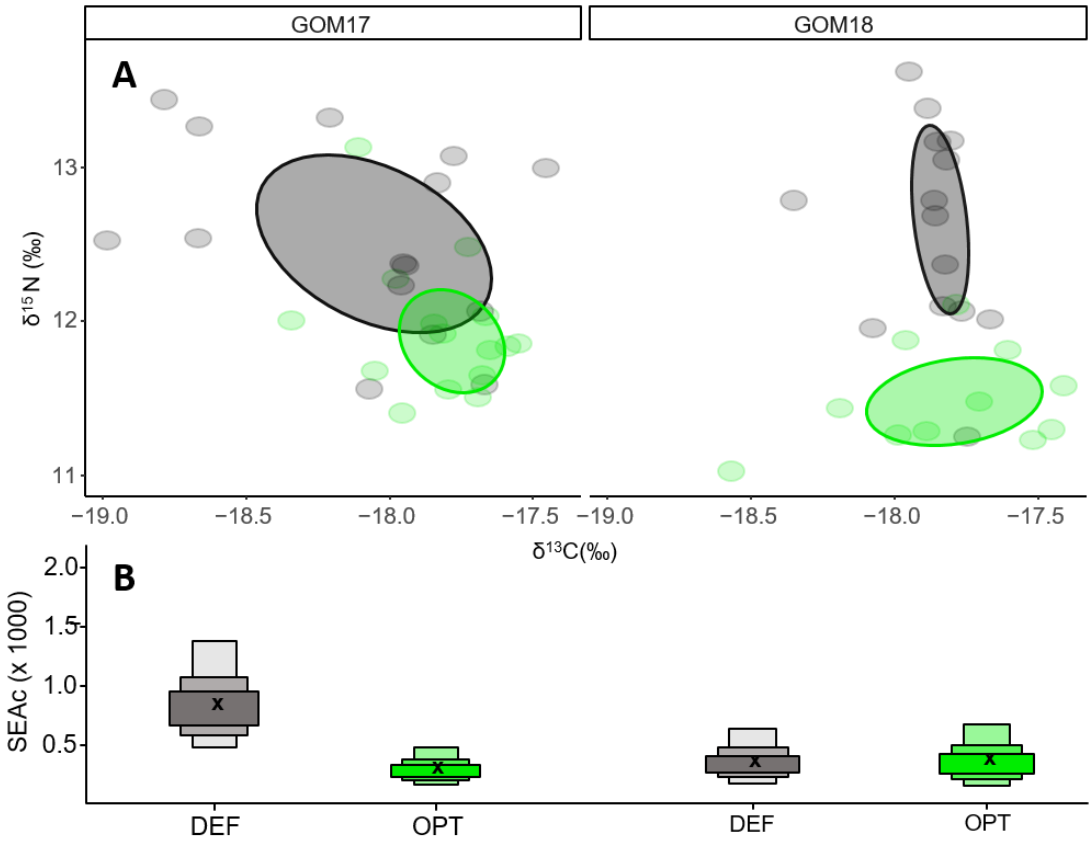

Figure 4. - (A) $\delta^{15}N$ vs $\delta^{13}C$ maternal values OPT (green) and DEF (grey) larvae for GOM17 and GOM18. The ellipses represent areas of maternal trophic niches. (B) Areas of the trophic niches estimated by for OPT and DEF groups. The cross represents size of the ellipse by applying the correction for small sample sizes (SEAc).

Larval Trophic Niches

Comparing inter-population trophic niches, we observed significant differences in both $\delta^{15}N$ and $\delta^{13}C$ between years (Table A1), without overlap of niche ellipses (Figure 5A). GOM18 larvae had larger trophic niches (0.58) than GOM17 larvae (0.23) (Figure 5B). At the intra-population level, OPT and DEF of both years did not differ in $\delta^{15}N$ values (Table A2). In contrast, $\delta^{13}C$ values differed between OPT and DEF for GOM18 (Figure 6A and Table A2). The trophic niches of OPT and DEF larvae for GOM17 overlap 36% (0.13) (Figure 6A), with similar niche sizes for both groups (0.25 OPT vs 0.23 DEF) (Figure 6B). OPT and DEF larvae for GOM18 have niche overlap of 19% (0.13) (Figure 6A), with larger areas for DEF (0.53) than OPT (0.28) (Figure 6B).

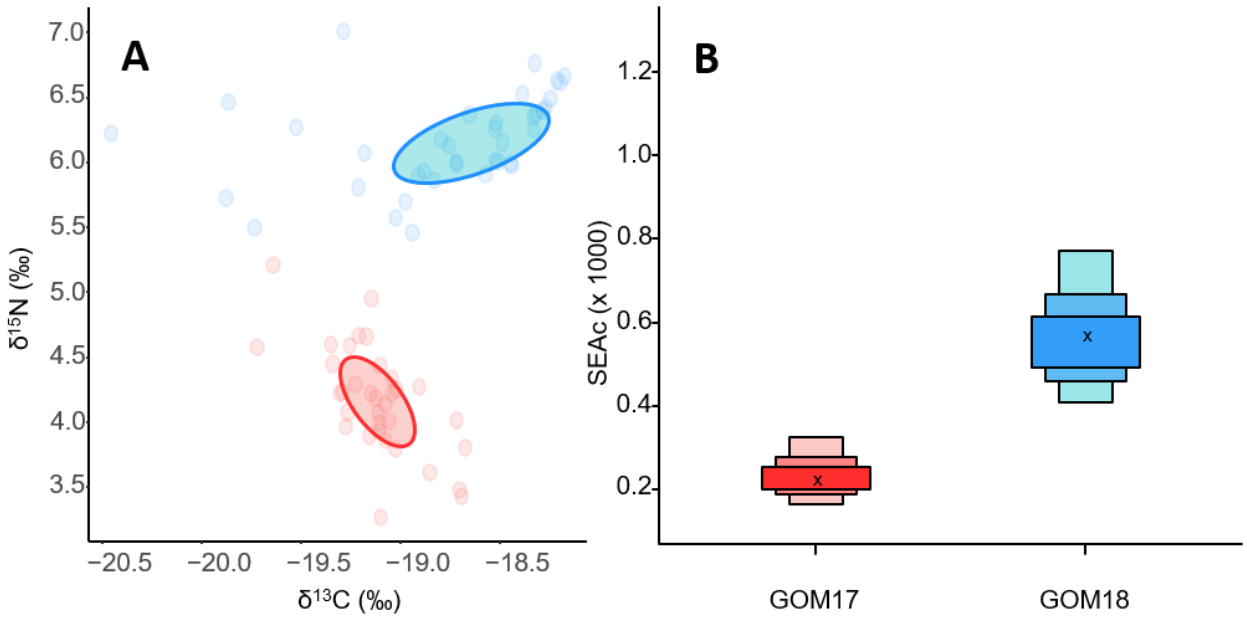

Figure 5. - (A) $\delta^{15}N$ vs $\delta^{13}C$ larval values for post-flexion larvae of GOM17 and GOM18. The ellipses represent the areas of the larval trophic niches estimated for each campaign. (B) Areas of the trophic niches estimated by SIBER of each GOM17 (0.23) and GOM18 (0.58) campaign. The cross represents the size of the ellipse by applying the correction for small sample sizes (SEAc).

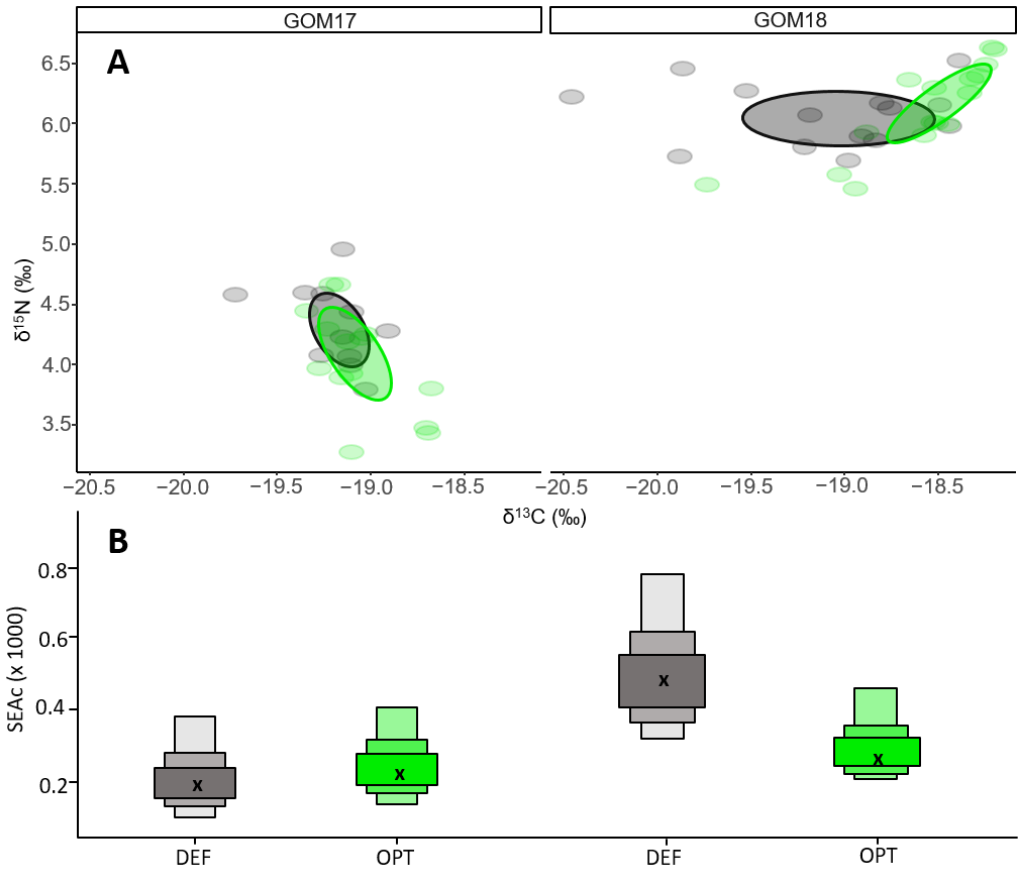

Figure 6. - (A) $\delta^{15}N$ vs $\delta^{13}C$ larval values OPT (green) and DEF (grey) larvae of GOM17 and GOM18 campaigns. Ellipse areas represent larval trophic niches. (B) Trophic niche areas estimated by SIBER with the correction for small sample sizes (SEAc).

Discussion

Larval fish growth during early development is closely linked to their survival [73]. With increasing size larvae become more adept at escaping predators and at catching larger more nutritious prey and ward off starvation [74,75]. Thus, the quicker the larvae grow, shortening the duration of this critical period of their lives the lower the cumulative mortality during the larval stage [76,77].

Larval growth is characterized by great plasticity, which is reflected in its variability depending on environmental characteristics [78], with temperature and food availability the most decisive factors for larval growth [79,32-35]. Temperature is an important factor for larval survival of the genus *Thunnus sp* [39,80] and especially influential for early developmental of ABFT [81,82]. GOM18 larvae experienced warmer temperature (Table 2) and showed higher somatic growth (SL and DW) and larger otolith biometrics (RAD and MIW) (Table 3). However, the temperature differences between GOM17 and GOM18 was relatively small, only 0.84ºC on average, so is unlikely to be the main reason for differences in observed growth patterns [83,57]. In previous studies of the same species, no growth pattern differences were detected among years with temperature differences exceeding 1ºC [34].

More likely, the inter-annual differences in growth rates would be better explained by differences in trophic dynamics [83] or genetic factors associated with maternal inheritance [66].

Concentrations of mesozooplankton (0.2 - 1 mm) were higher for GOM18 [67] than GOM17, which could suggest a cause-effect relationship between potential food availability trophodynamic and growth variability. Field studies indicated that environmental factors account for less than 40% of the variability observed in larval growth [85, 86], which suggests the importance of other factors such as genetic heritance. Maternal stable isotope transmission has been traced in perciforms to offspring [56]. Few studies have applied stable isotopes to investigate the effects of maternal nutrition on offspring quality [87]. Uriarte et al. [54] showed in a rearing experiment that eggs and pre-flexion larvae of eastern ABFT larvae reflected to the adult female isotopic signatures. For ABFT maternal influence analyzed from the changes in N isotopic values during pre-flexion stages has a decisive importance for larval growth [66]. This maternal effect gradually disappears with development until the values of the N and C isotope reaches steady state with exogenous feeding in post-flexion larvae. Therefore, to analyze the factors that determine the ABFT larval growth, it is useful to consider pre (greater maternal influence) and post-flexion (greater trophic influence) stages separately [54,55,15].

Maternal influence (pre-flexion larvae)

The maternal effect influences size at hatch and subsequent growth [88], thereby increasing larval viability and decreasing mortality [37,89,56]. The decreasing values of $\delta^{15}N$ with pre-flexion age, together with an increasing $\delta^{13}C$ profile for both GOM17 and GOM18 populations agree with observations for the same species both in culture experiments [54] and in field studies [55,15,66] The estimated maternal isotopic signatures ($\delta^{15}N_{maternal}$, $\delta^{13}C_{maternal}$) based on the equations of isotopic values with age in our field-collected samples (Table 1) showed no differences between years (Table 5) and the values are comparable to the isotopic signatures previously reported for adult muscle tissue [90-94,82]

Maternal trophic niches express the isotopic characteristics of the trophic niches exploited by the breeders. Their size can vary depending on food availability [95]. According to our results, the maternal isotopic niche areas were similar between years (Figure 3B) with a high degree of overlap (Figure 3A) which we interpret as that the females feeding on prey with similar mean isotopic characteristics. Our results do not mean that the spawning adults in both years came for exactly the same geographic locations, but they do support the "common feeding grounds" hypothesis [10] by which adults aggregate in large groups to feed broadly in the western Atlantic Ocean [8,96,97].

Therefore, at the population level, it does not seem that growth differences for pre-flexion stages (Figure A3 and Table 3) were related to differences in maternal isotopic niches or breeder trophic behavior. However, a direct relationship between maternal inheritance and larval growth can be evaluated by considering the contrasting growth groups in residual analysis [72,66].

According to our intra-population comparison, OPT growing larvae showed lower estimated maternal $\delta^{15}N$ values in both years (Table 4), implying a direct relationship between growth potential and maternal inheritance. This variability in maternally inherited $\delta^{15}N$ values may be based on various factors such as differences in age, condition, or natural variability in quality of spawning episodes [66].

In the GOM, ABFT is considered an opportunistic and generalist predator [92] that feeds on a wide range of available prey, and its diet is affected by food availability. The smaller maternal isotopic niches estimated for GOM2017 OPT larvae (Figures 4A and 4B) could be associated with a more selective maternal diet on a low number of species [98]. On the other hand, the wider maternal isotopic niches for DEF suggest a more diverse diet and generalist trophic behavior. As trophic niches sizes are related to ecosystem productivity [99], consumers must adapt foraging strategy in order to satisfy their metabolic demands. Following this reasoning, larvae with greater growth potential would seem to be associated with more stenophagous maternal trophic behavior in which females cover their energy requirements with more selective feeding behavior in areas of greater production and as a likely result higher quality prey. In contrast, those with lower growth potential would be associated with maternal euryphagous behaviors in which females search for food over larger less-productive areas.

Since 2018 OPT and DEF larvae had similar maternal niches widths, growth differences between these groups cannot be associated with differences in the breeder trophic behavior as for GOM17 (Figures 4A and AB). Moreover, the absence of overlap of maternal niches between these groups (Figures 4A and 4B) could be due to many factors that determine N isotopic signature such as age, nutritional status and quality variance among/within spawning batches previously mentioned. Further investigations are needed to elucidate the implications of these various factors for larval growth variability.

Trophic behavior (post-flexion larvae)

$\delta^{15}N$ levels are enriched with each trophic transfer, providing information about the TPs of consumers [51,100]. In previous studies, better larval growth was found to be associated with higher TPs [101,57,65], which was interpreted as reflecting greater trophic specialization. According to our results, however, larvae with better growth from GOM18 had lower TPs than GOM17 (Table A1). Similar observations have been reported for larval Shortbelly Rockfish where larvae with a lower TP were heavier and grew faster [102]. TP reflects how the energy gets transfer from the base of the food web up to the larva [100,103] and its estimation can be influenced by food chain efficiency [105,104], which causes a wide range of TP estimates in the GOM [65].

ABFT larvae develop in oligotrophic ecosystems [10]. The main trophic pathway through such microbially dominated systems is highly inefficient, with most production lost to bacterial remineralized and multi-step protistan food chains [106]. Knapp et al. [107] found that N_2 fixation accounted for a relatively small component of new N-based productivity during GOM17 and GOM18, and Kelly et al. [26] observed that chronic N deficits in the offshore oligotrophic waters where ABFT larvae live are met by lateral advection of organic matter from the more productive shelf regions. The average contribution of nitrogen fixation was double in GOM17 compared to GOM18, while the advected particulate organic nitrogen (PON) was 5 times higher in GOM18 [105]. Thus, greater oligotrophy in 2017 could explain the unusually depleted values of $\delta^{15}N$ observed from micro- and meso-zooplankton (Table 2) to ABFT larvae (Table A1).

Our results are consistent with those summarized by Gerard et al. [64] for the BLOOFINZ-GOM cruises, suggesting ABFT larvae are more likely to thrive by feeding at

a lower trophic position regardless of the source of production (GOM18). These findings appear consistant with the newly proposed Trophic Efficiency in Early Life hypothesis which states that in order to survive larvae must feed on prey that are low in the food chain thereby maximising energy transfer from the food chain base sustaining the larval population [104] (Figure A2 and Table 3).

ABFT larvae are daylight visual feeders that feed selectively on preferred prey such as copepods, copepod nauplii, appendicularians and cladocerans [44,45,108,109,46,67]). Stukel et al. [105] indicated that a ABFT diet of calanoid copepods and podonid cladocerans (which were more abundant in the water column during GOM18), was consistent with maintaining relatively low trophic positions. Likewise, Shiroza et al. [46] demonstrated that highly selective predation on cladoceran was an active process, which would support the idea that ABFT larvae are highly specialized for maximizing trophic efficiency in the oligotrophic environments where they develop.

In the inter-annual comparison, the larvae occupy completely separate isotopic niche areas (Figure 5A), which would imply that they exploit trophic niches with very different isotopic characteristics depending on the year. Zooplankton biomass was higher with greater diversity and concentrations of preferred ABFT larval prey in GOM18 compared to GOM17 [110,46]. The greater growth observed in 2018 would be associated with larger larval trophic niches that would reflect the greater availability of preferred prey, facilitating higher growth rates [67]. Conversely, the lower concentration and richness of prey (including preferred types) in 2017 could result in narrower isotopic niches (Fig 5B) being, from a trophic point of view, a limiting situation for development reflected in lower growth rates. In this case, inter-population growth differences in post-flexion stages would be associated with the aforementioned differences in food availability and diversity rather than with trophic behavior shifts.

The intra-population analysis of isotopic niches offers different results for each group. In 2018, larvae with optimal growth are associated with narrower trophic niches, which can be interpreted as more selective trophic behavior in higher production ecosystem (Figures 6A and 6B). At this point it is important to highlight that the trophic niche differences between OPT and DEF are determined mainly by the range of variation in $\delta^{13}C$ values, which reflect the prey carbon sources for larval growth. In this sense, trophic niche size of OPT may rely more on food chains fueled by production from laterally transported water masses, which one might expect have a higher $\delta^{13}C$ signature [111,105].

On the other hand, the similarities of isotopic niches with respect to their widths and their high degree of overlap for GOM17 do not explain the observed larval growth differences between OPT and DEF groups for this year based on trophic reasons (Figures 6A and 6B). This could be one area better explained by maternal inheritance. This inter-generational transfer tracked through the $\delta^{15}N$ values would arise from trophic characteristics of breeders [66] that may influence larval growth into the flexion stage. Moreover, it cannot be ruled out that the suboptimal larval feeding conditions and more homogeneous oligotrophic environment due to less lateral transport [110,105] prevents us from statistically separating OPT and DEF based on their isotopic niches.

C:N ratio has been used to evaluate nutritional status [112], being a particularly good proxy for the amount of lipid reserve [68]. For the intra-population comparison, C:N values were consistently higher in larvae with lower growth potential in both years and regardless of developmental stage (Figure 2 and Table A3). We interpret these results as a lower consumption of lipid reserves for growth by DEF larvae, unlike the OPT growth group whose lipid levels are reduced as a consequence of a greater energy investment in somatic growth.

Conclusions

Our results corroborate that there is a direct relationship between growth potential and $\delta^{15}N$ signatures for ABFT pre-flexion larvae due to feeding behavior of the breeders

that is passed down maternal heritance. Moreover, the estimation of ABFT maternal isotopic signatures and isotopic niche space based on the isotopic signatures of size at age of pre-flexion larvae are consistent with previous SIA studies that also utilized muscle tissue of adult females.

Larval trophic ecology was shown to follow the availability and diversity of prey reflected in their isotopic niches widths and overlaps, which influenced larval growth potential. TP estimates determined by food web length/efficiency and can lead to substantial range in these estimates with temporal and spatial variability in trophic conditions. Regardless of development status, larvae with higher growth potential showed significantly lower C:N, consistent with greater energy investment in growth.

Author Contributions: Conceptualization J.M.Q. and R.L.C.; Methodology J.M.Q, R.B.S, E.M. and R.L.C. Formal analysis J.M.Q., R.B.S., E.M. and R.L.C., Investigation J.M.Q., R.B.S., E.M. and R.L.C. Resources J.M.Q., R.B.S., E.M. and R.L.C. Writing - Original Draft Writing J.M.Q., R.B.S., EM, R.S., M.R.L., T.G., J.L., A.G. and R.L.C. Writing - Review & Editing J.M.Q., R.B.S., E.M., R.S., M.R.L., T.G., J.L. A.G. and R.L.C. Visualization J.M.Q., R.B.S., E.M. and R.L.C. Supervision J.M.Q. and R.L.C. Project

their support in conducting the field GOM sampling during both years. We acknowledge.administrator M.R.L. and R.L.C., Funding acquisition M.R.L., J.L. and R.L.C.

Funding: BLOOFINZ funding from projects NOAA-NOS-NCCOS-2017-2004875 and NA15OAR4320 071 of the NOAA RESTORE Science Program and US National Science Foundation grants OCE-1851558 and -1851395 and ECOLATUN (CTM-2015-68473-R MINECO/FEDER) projects from the Spanish Ministry of Economy and Competitiveness and Cooperative Institute for Marine and Atmospheric Studies (#NA20OAR4320472).

Institutional Review Board Statement: Not applicable.

Informed Consent Statement: Not applicable.

Data Availability Statement: Data supporting the results stated above can be sent to anyone requesting them from the authors.

Acknowledgments: We thank the crew of the National Oceanic and Atmospheric Administration (NOAA) ship R/V Nancy Foster for

Conflicts of Interest: The authors declare no conflict of interest.

APPENDIX 1

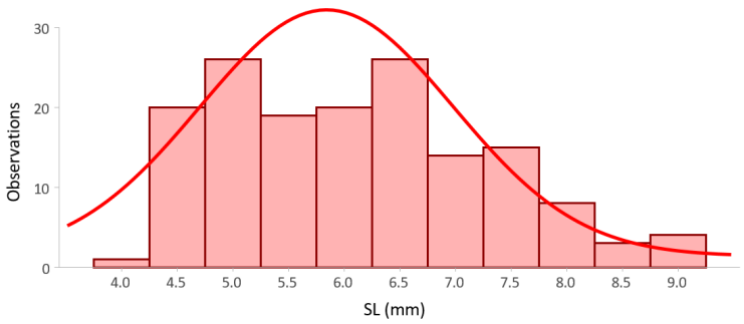

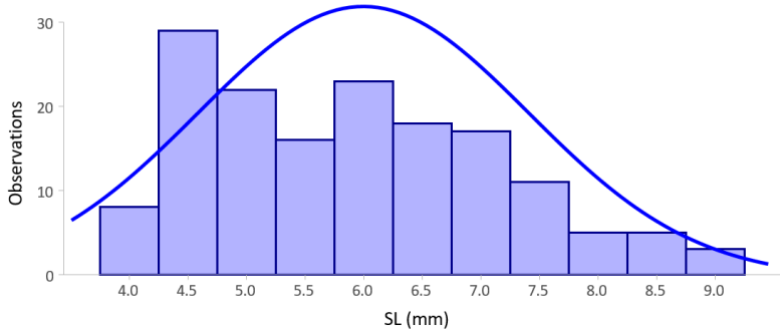

Figure A1. - Histogram of frequencies of the different sizes for GOM17 (red) and GOM18 (blue) sampling years.

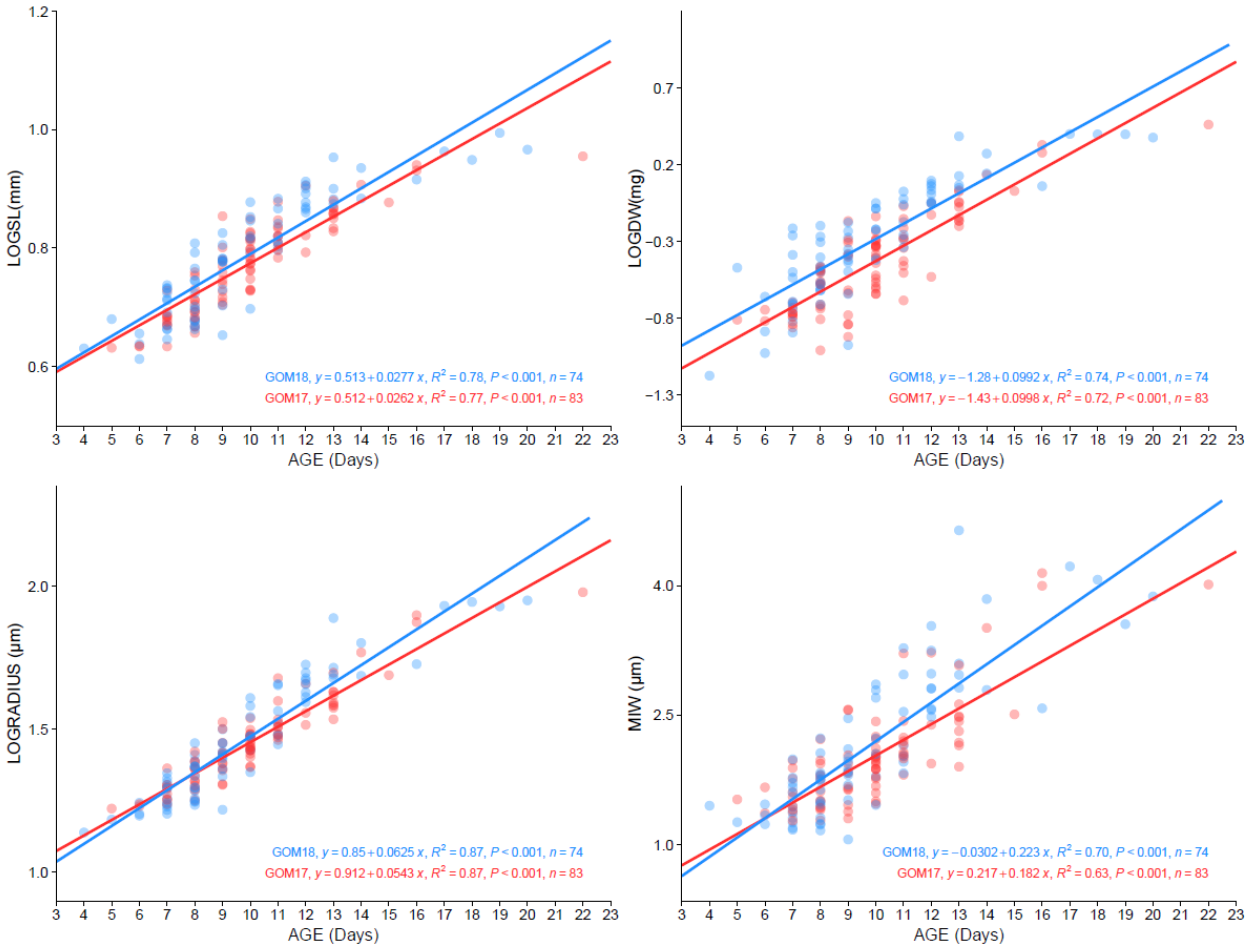

Figure A2. - Comparison of somatic growth pattern (LOGSL, LOGDW) and biometric of otoliths (LOGRADIO, MIW) between years (GOM17 (red), GOM18 (blue)) versus AGE. The equations coefficients and R^2 are included.

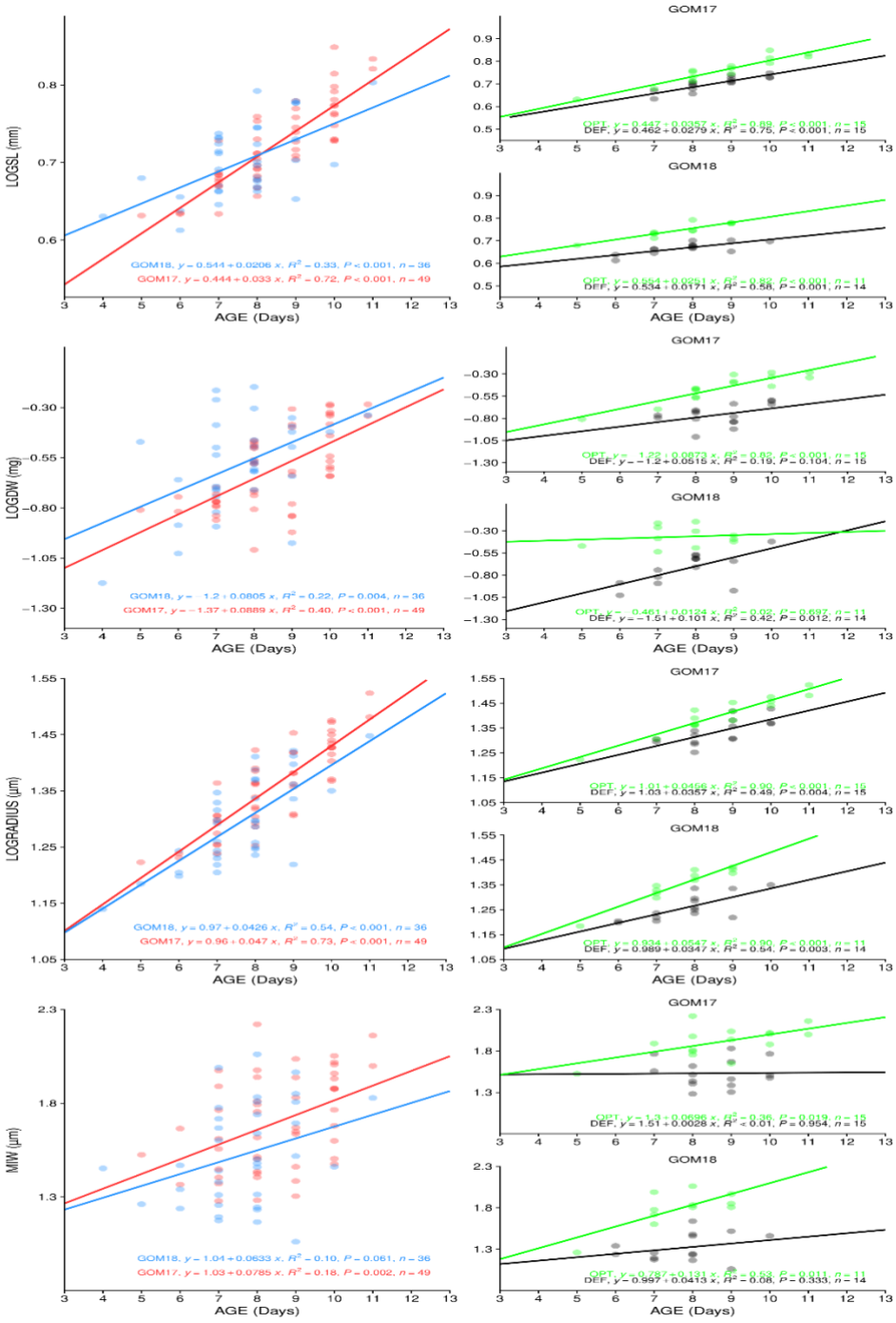

Figure A3. - Comparison of somatic (LOGSL, LOGDW) and otoliths biometrics (LOGRADIO, MIW) versus AGE of pre-flexion larvae according to inter-population (GOM17 in red, GOM18 in blue) and intra-population (OPT in green, DEF in black). The equations coefficients and R^2 are included.

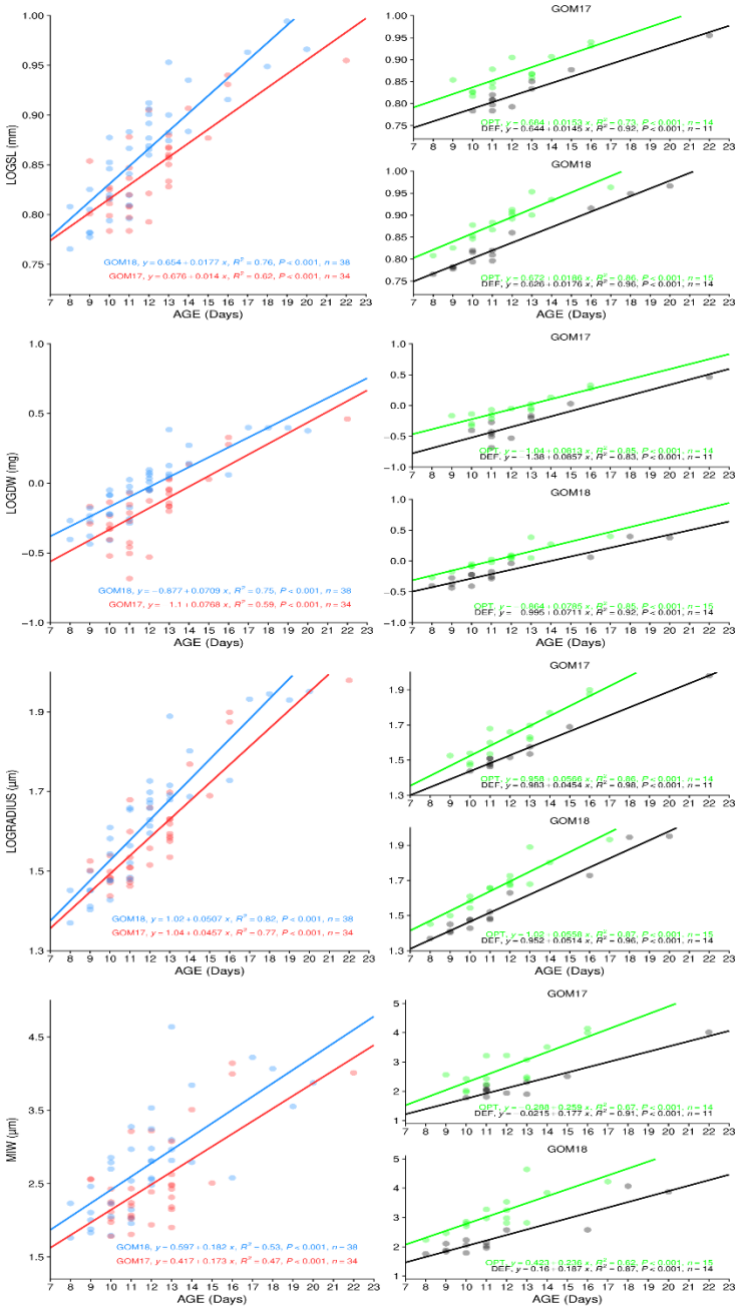

Figure A4. - Comparison of somatic (LOGSL, LOGDW) and otoliths biometric (LOGRADIO, MIW) versus AGE, of post-flexion larvae according to inter-population analysis between years (GOM17 in red, GOM18 in blue) and intra-population (OPT in green, DEF in black). The equations coefficients and R^2 are included.

Table A1. - $\delta^{15}N$, $\delta^{13}C$, C:N and TP in inter-population level grouping by stage (PRE, POST, TOTAL) of each campaign (GOM17,GOM18). ANCOVA analysis result (F, p) using AGE as covariate and ANOVA results. NS= Non-significant; * $p < 0.05$; ** $p < 0.01$.

		GOM17				GOM18				ANCOVA		ANOVA	
		N	MIN	MAX	MEDIA ± SD	N	MIN	MAX	MEDIA ± SD	$F_{1,154}$	*p*	$F_{1,154}$	*p*
TOTAL	$\delta^{15}N$	83	3.27	6.16	4.47 ± 0.59	74	5.46	9.04	6.60 ± 0.78	454.78	**		
	$\delta^{13}C$		-20.3	-18.1	-19.1 ± 0.34		-20.5	-18.2	-18.8 ± 0.42			37.02	**
	CN		3.62	4.96	4.20 ± 0.27		3.86	7.97	4.40 ± 0.54	9.19	**		
		N	MIN	MAX	MEDIA ± SD	N	MIN	MAX	MEDIA ± SD	$F_{1,82}$	*p*		
PRE	$\delta^{15}N$	49	3.51	6.16	4.68 ± 0.61	36	5.72	9.04	7.06 ± 0.85	197.89	**		
	$\delta^{13}C$		-20.3	-18.1	-19.1 ± 0.40		-19.4	-18.4	-18.8 ± 0.23	21.6	**		
	CN		3.93	4.96	4.33 ± 0.26		3.95	5.01	4.42 ± 0.27	0.602	NS		
		N	MIN	MAX	MEDIA ± SD	N	MIN	MAX	MEDIA ± SD	$F_{1,69}$	*p*	$F_{1,69}$	*p*
POST	$\delta^{15}N$	34	3.27	5.21	4.17 ± 0.42	38	5.46	7.00	6.16 ± 0.35			474.88	**
	$\delta^{13}C$		-20	-19	-19.10 ± 0.23		-20.5	-18.20	-18.80 ± 0.54	13.137	**		
	CN		3.62	4.3	4.01 ± 0.14		3.86	7.97	4.37 ± 0.71	8.786	**		
	TP(1.46)		3.77	5.10	4.38 ± 0.29		3.17	4.23	3.65 ± 0.24			136.49	**

Table A2. - $\delta^{15}N$, $\delta^{13}C$, C:N and TP in intra-population level grouping by stage (PRE, POST, TOTAL) and growth (OPT,DEF) of each campaign (GOM17,GOM18). ANCOVA analysis result (F, p) using AGE as covariate and ANOVA results. NS= Non-significant; * $p < 0.05$; ** $p < 0.01$.

			OPT(+)				DEF(-)				ANCOVA		ANOVA	
			N	MIN	MAX	MEAN ± SD	N	MIN	MAX	MEAN ± SD	$F_{1,52}$	*p*	$F_{1,52}$	*p*
	GOM17	$\delta^{15}N$		3.43	4.67	4.15 ± 0.33		3.79	5.86	4.75 ± 0.56	19.83	***		
		$\delta^{13}C$	27	-19	-19	-19.1 ± 0.20	28	-20.3	-18.1	-19.2 ± 0.46	2.626	NS		
		CN		3.76	4.30	4.05 ± 0.13		3.62	4.96	4.33 ± 0.31	18.31	***		
TOTAL			N	MIN	MAX	MEAN ± SD	N	MIN	MAX	MEAN ± SD	$F_{1,59}$	*p*	$F_{1,59}$	*p*
	GOM18	$\delta^{15}N$		5.46	7.69	6.26 ± 0.46		5.69	9.04	6.95 ± 0.93	19.68	***		
		$\delta^{13}C$	36	-19.9	-18.2	-18.7 ± 0.40	26	-19.9	-18.3	-18.8 ± 0.31			0.23	NS
		CN		3.86	5.01	4.26 ± 0.28		3.92	5.79	4.44 ± 0.39	5.324	*		
			N	MIN	MAX	MEAN ± SD	N	MIN	MAX	MEAN ± SD	$F_{1,27}$	*p*	$F_{1,27}$	*p*
	GOM17	$\delta^{15}N$		3.82	5.55	4.33 ± 0.44		3.96	5.86	4.94 ± 0.59			10.09	**
		$\delta^{13}C$	15	-19.4	-18.8	-19.1 ± 0.18	15	-20.3	-18.8	-19.4 ± 0.47			3.985	NS
		CN		4.04	4.66	4.20 ± 0.17		4.06	4.82	4.43 ± 0.25			8.317	**
PRE			N	MIN	MAX	MEAN ± SD	N	MIN	MAX	MEAN ± SD	$F_{1,23}$	*p*	$F_{1,23}$	*p*
	GOM18	$\delta^{15}N$		5.72	7.69	6.50 ± 0.56		6.06	9.04	7.53 ± 0.84	24.81	***		
		$\delta^{13}C$	11	-19.4	-18.4	-18.7 ± 0.29	14	-19.0	-18.4	-18.7 ± 0.18			0.148	NS
		CN		3.95	5.01	4.36 ± 0.21		4.07	4.97	4.51 ± 0.29			1.71	NS
			N	MIN	MAX	MEAN ± SD	N	MIN	MAX	MEAN ± SD	$F_{1,26}$	*p*	$F_{1,26}$	*p*
	GOM17	$\delta^{15}N$		3.27	4.67	4.04 ± 0.44		3.79	4.95	4.33 ± 0.34			3.32	NS
		$\delta^{13}C$	14	-19.3	-18.7	-19.1 ± 0.22	11	-19.7	-18.9	-19.2 ± 0.21			2.37	NS
		CN		3.74	4.30	3.98 ± 0.15		3.62	4.20	4.03 ± 0.16	4.74	*		
		TP(1.46)		3.77	4.72	4.29 ± 0.30		4.13	4.92	4.49 ± 0.23			3.32	NS
POST			N	MIN	MAX	MEAN ± SD	N	MIN	MAX	MEAN ± SD	$F_{1,26}$	*p*	$F_{1,26}$	*p*
	GOM18	$\delta^{15}N$		5.46	6.63	6.10 ± 0.39		5.69	6.52	6.07 ± 0.26			0.078	NS
		$\delta^{13}C$	15	-19.7	-18.2	-18.6 ± 0.41	14	-20.5	-18.4	-19.1 ± 0.61	9.72	**		
		CN		3.86	4.94	4.14 ± 0.26		3.92	7.97	4.73 ± 1.06			4.76	*
		TP(1.46)		3.17	3.97	3.61 ± 0.27		3.33	3.90	3.59 ± 0.18			0.078	NS

References

1. Bakun, A.; Broad, K.. Environmental 'loopholes' and fish population dynamics: comparative pattern recognition with focus on El Nino effects in the Pacific. *Fish. Oceanogr* (2003). *12*, 458–473. [CrossRef]
2. Bakun, A. Fronts and eddies as key structures in the habitat of marine fish larvae: opportunity, adaptive response and competitive advantage. *Sci. Mar* (2006). 70, 105–122. [CrossRef]
3. Pauly, D.; Christensen, V.; Dalsgaard, J.; Froese, R.; Torres, F.C. Fishing down marine food webs. *Science* (1998), 279:860– 863. [CrossRef]

4. Essington, T.E.; Schindler, D.E.; Olson, R.J.; Kitchell, J.F.; Boggs, C.; Hilborn, R. Alternative fisheries and the predation rate of yellowfin tuna in the eastern pacific ocean. *Ecological Applications* (2002), 12: 724-734. [CrossRef]
5. Scheffer, M.; Carpenter, S.; Bd, Y. Cascading effects of overfishing marine systems. *Trends Ecol. Evol* (2005), 20:579–581. [CrossRef]
6. Rooker, J.R.; Alvarado Bremer, J.R.; Block, B.A.; de Metrio, G.; Corriero, A.; Krause, R.T.; Prince, E.D.; Rodriguez-Marin, E.; Secor, D.H. Life history and stock structure of Atlantic bluefin tuna (*Thunnus thynnus*). *Rev Fish Sci* (2007), 15, 265–310. [CrossRef]
7. Carlsson, J.; McDowell, JR.; Carlsson, JE.; GRAVES, JE. Genetic identity of YOY bluefin tuna from the eastern and western Atlantic spawning areas. *Journal of Heredity* (2007), 98(1), 23-28. [CrossRef]
8. Rooker, J.R.; Secor, D.H.; DeMetrio, G.; Kaufman, A.J.; Ríos, A.B.; Ticina, V. Evidence of trans-Atlantic movement and natal homing of bluefin tuna from stable isotopes in otoliths. *Mar. Ecol. Prog. Ser* (2008), 368, 231–239. [CrossRef]
9. Johnstone, C.; Pérez, M.; Malca, E.; Quintanilla, J.M.; Gerard, T.; Lozano-Peral, D.; Alemany, F.; Lamkin, J.; García, A.; Laiz-Carrión, R. Genetic connectivity between Atlantic bluefin tuna larvae spawned in the Gulf of Mexico and in the Mediterranean Sea. *PeerJ 9:e11568* (2021). [CrossRef]
10. Muhling, B.A.; Lamkin, J.T.; Alemany, F.; García, A.; Farley, J.; Ingram Jr, G.W.; Alvarez Berastegui, D.A.; Reglero, P.; Carrión, R. Reproduction and larval biology in tunas, and the importance of restricted area spawning grounds. *Rev. Fish Biol. Fisheries* 27 (2017), 697–732. [CrossRef]
11. Deshpande, A.D.; Dickhut, R.M.; Dockum, B.W.; Farrington, C.; Brill, R.W. Polychlorinated biphenyls and organochlorine pesticides as intrinsic tracer tags of foraging grounds of bluefin tuna in the Northwest Atlantic Ocean. *Mar Pollut. Bull* (2016), 105(1), 265-276. [CrossRef]
12. Druon, J.N.; Fromentin, J.M.; Hanke, A.; Arrizabalaga, H.; Damalas, D.; Ticina, V.; Quílez-Badia, G.; Ramirez, K.; Arregui, I.; Tserpes, G.; Reglero, P.; Deflorio, M.; Oray, I.; Karulak, F.S.; Megalofonou, P.; Ceyhan, T.; Grubisic, L.; MacKenzie, B.R.; Lamkin, J.; Addis, P. Habitat suitability of the Atlantic bluefin tuna by size class: An ecological niche approach. *Prog. Oceanogr* (2016), 142, 30-46. [CrossRef]
13. ICCAT. Report of the 2019 Intersessional Meeting of the ICCAT Bluefin Tuna Species Group. Collect. Vol. Sci. Pap. *ICCAT* (2019), 76(2), 1–70. [CrossRef]
14. Puncher, G.N.; Hanke, A.; Busawon, D.; Sylvester, E.V.A.; Golet, W.; Hamilton, L.C.; Pavey, S.A. Individual assignment of Atlantic bluefin tuna in the northwestern Atlantic Ocean using single nucleotide polymorphisms reveals an increasing proportion of migrants from the eastern Atlantic Ocean. *Can. J. Fish. Aquat. Sci* (2022), 79(1), 111-123. [CrossRef]
15. Laiz-Carrión, R.; Gerard, T.; Suca, J.J.; Malca, E.; Uriarte, A.; Quintanilla, J.M.; Privoznik, S.L.; Llopiz, J.K.; et al. Stable isotope analysis indicates resource partitioning and trophic niche overlap in larvae of four tuna species in the Gulf of Mexico. *Mar. Ecol. Prog. Ser* (2019), 619:53-68. [CrossRef]
16. Medina, A. Reproduction of Atlantic bluefin tuna. *Fish Fisheries* (2020), 21, 1109– 1119. [CrossRef]
17. Alemany, F.; Quintanilla, L.; Velez-Belchi, P.; García, A.; Cortés, D.; Rodróguez, J.M.; Fernández de Puelles, M.L.; González-Pola, C.; López-Jurado, J.L. Characterization of the spawning hábitat of atlantic bluefin tuna and related species in the Balearic Sea (western Mediterranean). *Prog. Oceanogr* (2010), 86, 21-38. [CrossRef]
18. Fahnenstiel, G.; Mccormick, M. J.; Lang, G. A.; Redalje, D. G.; Lohrenz, S. E.; Markowitz, M.; Wagoner, B.; Carrick, H. J. Taxon-specific growth and loss rates for dominant phytoplankton populations from the northern Gulf of Mexico. Mar. *Ecol. Prog. Ser* (1995), 117, 229–239. [CrossRef]
19. Rabalais, N.; Turner, R. E.; Dortch, Q.; Justic, D.; Bierman, V.JR.; WISEMAN, W. JR. Nutrient-enhanced productivity in the northern Gulf of Mexico: past, present and future. *Hydrobiologia* (2002), 475/476, 39–63. [CrossRef]
20. Lohrenz, S. E.; Redalje, D. G.; Cai, W. J.; Acker, J.; Dagg, M. A retrospective analysis of nutrients and phytoplankton productivity in the Mississippi River plume. *Cont. Shelf Res* (2008), 28, 1466–1475. [CrossRef]
21. Liu, H.; Dagg, M. Interactions between nutrients, phytoplankton growth, and micro- and mesozooplankton grazing in the plume of the Mississippi River. *Mar. Ecol. Prog. Ser* (2003), 258, 31–42. [CrossRef]
22. Qian, Y.; Jochens, A.E.; Kennicutt, M.C. II.; Biggs, D.C. (2003) Spatial and temporal variability of phytoplankton biomass and community structure over the continental margin of the Northeast Gulf of Mexico based on pigment analysis. *Cont. Shelf Res* (2003), 23, 1–17. [CrossRef]
23. Wawrik, B.; Paul, J. H. Phytoplankton community structure and productivity along the axis of the Mississippi River plume in oligotrophic Gulf of Mexico waters. *Aquat. Microb. Ecol* (2004), 35, 185–196. [CrossRef]
24. Biggs, D. C.; Müller-Karger, F. E. Ship and satellite observations of chlorophyll stocks in interacting cyclone-anticyclone eddy pairs in the western Gulf of Mexico. *J. Geophys. Res. Oceans* (1994), 99, 7371–7384. [CrossRef]
25. Hidalgo-González, R. M.; Alvarez-Borrego, S.; Fuentes-Yaco, C.; Platt, T. Satellite-derived total and new phytoplankton production in the Gulf of Mexico. *Indian J. Mar. Sci*. (2005), 34, 408–417.

26. Kelly, T.B.; Knapp, A.N.; Landry, M.R. et al. Lateral advection supports nitrogen export in the oligotrophic open-ocean Gulf of Mexico. *Nat Commun* (2021), 12, 3325. [CrossRef]
27. Lindo-Atichati, D.; Bringas, F.; Goni, G.; Muhling, B.; Muller-Karger, F. E.; Habtes, S. Varying mesoscale structures influence larval fish distribution in the northern Gulf of Mexico. *Mar Ecol Prog Ser* (2012), 463, 245-257. [CrossRef]
28. Vukovich, F. M. Climatology of ocean features in the Gulf of Mexico using satellite remote sensing data. *J. Phys. Oceanogr* (2007), 37, 689–707. [CrossRef]
29. Bracco, A.; Choi, J.; Joshi, K.; Luo, H.; McWilliams, J. C. Submesoscale currents in the northern Gulf of Mexico: deep phenomena and dispersion over the continental slope. *Ocean Model* (2016), 101, 43–58. [CrossRef]
30. Bakun, A. Ocean eddies, predator pits and bluefin tuna: implications of an inferred 'low risk–limited payoff' reproductive scheme of a (former) archetypical top predator. *Fish Fish* (2013), 14, 424-438. [CrossRef]
31. Muhling, B. A.; Lamkin, J. T.; Roffer, M. A. Predicting the occurrence of bluefin tuna (*Thunnus thynnus*) larvae in the northern GOM: Building a classification model from archival data. *Fish. Oceanogr* (2010), 19, 526–539. [CrossRef]
32. Tanaka, Y.; Satoh, K.; Iwahashi, M.; Yamada, H. Growth dependent recruitment of Pacific bluefin tuna (*Thunnus orientalis*) in the northwestern Pacific Ocean. *Mar Ecol Prog Ser* (2006), 319, 225–235. [CrossRef]
33. Wexler, J.B.; Chow, S.; Wakabayashi, T.; Nohara, K.; Margulies, D. Temporal variation in growth of yellowfin tuna (*Thunnus albacares*) larvae in the Panama Bight, 1990–97. *Fish. Bull* (2007), (1), 1–18. [CrossRef]
34. García, A.; Cortés, D.; Quintanilla, J.; Ramirez, T.; Quintanilla, L.; Rodrıíguez, J. M.; Alemany, F. Climate-induced environmental conditions influencing interannual variability of Mediterranean bluefin (*Thunnus thynnus*) larval growth. *Fish. Oceanogr* (2013), 22, 273–287. [CrossRef]
35. Satoh, K.; Tanaka, Y.; Masujima, M.; Okazaki, M.; Kato, Y.; Shono, H.; Suzuki, K. Relationship between the growth and survival of larval Pacific bluefin tuna, *Thunnus orientalis*. *Mar. Biol* (2013), 160, 691–702. [CrossRef]
36. Reglero, P.; Tittensor, D.P.; Álvarez-Berastegui, D.; Aparicio-González, A.; Worm, B. Worldwide distributions of tuna larvae: revisiting hypotheses on environmental requirements for spawning habitats. *Mar. Ecol. Prog. Ser* (2014), 501, 207-224. [CrossRef]
37. Chambers, R.C.; Leggett, W.C. Size and age at metamorphosis in marine fishes: an analysis of laboratory- reared winter flounder (Pseudopleuronectes americanus) with a review of variation in other species. *Can. J. Fish. Aquat. Sci* (1987), 44:1936–1947. [CrossRef]
38. Houde, E.D. Fish early life dynamics and recruitment variability. *American Fisheries Society Symposium Series* (1987), V.2:17–29. [CrossRef]
39. Kimura, S.; Kato, Y.; Kitigawa, T.; Yamaoka, N. Impacts of environmental variability and global warming scenario on Pacific bluefin tuna (Thunnus orientalis) spawning grounds and recruitment habitat. *Prog. Oceanogr* (2010), 86(1–2), 39-44. [CrossRef]
40. Suzuki, Z.; Kimoto, A.; Sakai, O. Note on the strong 2003 year-class that appeared in the Atlantic bluefin fisheries. Collect. *Vol. Sci. Pap. ICCAT* (2013), 69(1), 229-234. [CrossRef]
41. Costalago, D.; Tecchio, S.; Palomera, I.; Alvarez-Calleja, I.; Ospina-Alvarez, A.; Raicevich, S. Ecological understanding for fishery management: condition and growth of anchovy late larvae during different seasons in the Northwestern Mediterranean. *Est Coast Shelf Sci* (2011), 93, 350-358. [CrossRef]
42. Pepin, P.; Robert, D.; Bouchard, C.; Dower, J.F.; Falardeau, M.; Fortier, L.; Jenkins, G.P.; Leclerc, V.; Levesque, K.; Llopiz, J.K.; Meekan, M.G.; Murphy, H.M.; Ringuette, M.; Sirois, P.; Sponaugle, S. Once upon a larva: revisiting the relationship between feeding success and growth in fish larvae. *ICES J. Mar. Sci*. (2015), 72(2), 359-373. [CrossRef]
43. Cata, E.; Olivar, M.P.; Villate, F.; Uriarte, I. A comparison of anchovy (Engraulis encrasicolus) and sardine (Sardina pilchardus) larvae feeding in the Northwest Mediterranean: Influence of prey availability and ontogeny. *ICES J. Mar. Sci*. (2010), 67(5), 897-908. [CrossRef]
44. Catalán, I. A.; Tejedor, A.; Alemany, F.; Reglero, P. Trophic ecology of Atlantic bluefin tuna (Thunnus thynnus) larvae. *J. Fish Biol* (2011), 78, 1545–1560. [CrossRef]
45. Llopiz, J.K.; Muhling, B.A.; Lamkin, J.T. Feeding dynamics of Atlantic bluefin tuna (*Thunnus thynnus*) larvae in the Gulf of Mexico. *Col Vol Sci Pap ICCAT* (2015), 71, 1710–1715. [CrossRef]
46. Shiroza, A.; Malca, E.; Lamkin, J. T.; Gerard, T.; Landry, M. R.; Stukel, M. R., et al. Diet and prey selection in developing larvae of Atlantic bluefin tuna (*Thunnus thynnus*) in spawning grounds of the Gulf of Mexico. *J. Plank. Res* (2022), 44(5), 728–746. [CrossRef]
47. Logan, J.; Haas, H.; Deegan, L. et al. (2006). Turnover rates of nitrogen stable isotopes in the salt marsh mummichog, *Fundulus heteroclitus*, following a laboratory diet switch. *Oecologi*a (2006), 147, 391–395. [CrossRef]
48. Laiz-Carrion, R.; Cabrero, A.; Quintanilla, J.M.; Hernández, A.; Uriarte, A.; Gago, J.; Rodríguez, J.M.; Piñeiro, C.; García, A.; Saborido-Rey, F. Shifts in the seasonal trophic ecology of larvae and juveniles of European hake (Merluccius merluccius): From the Galician upwelling system (NW Spain). *Fish. Oceanogr* (2022), 31, 539–553. [CrossRef]

49. Minagawa, M.; Wada, E. Stepwise enrichment of δ15N along food chains: further evidence and the relation between δ15N and animal age. *Geochim Cosmochim Acta* (1984), 48, 1135−1140. [CrossRef]
50. Peterson, B.J.; Fry, B. Stable isotopes in ecosystem studies. *Ann. Rev. Ecol. Syst* (1987), 18, 293–320. [CrossRef]
51. Post, D.M. Using stable isotopes to estimate trophic position: models, methods, and assumptions. *Ecology* (2002), 83(3), 703-718. [CrossRef]
52. France, R.L.; Peters, R.H. Ecosystem differences in δ13C enrichment in aquatic foodwebs. *Can J Fish Aquat Sci* (1997), 54, 1255−1258. [CrossRef]
53. Laiz-Carrion, R.; Gerard, T.; Uriarte, A.; Malca, E.; Quintanilla, J.M.; Muhling, B.A.; Alemany, F.; Privoznik, S.L.; Shiroza, A.; Lamkin, J.T.; García, A. Trophic ecology of Atlantic bluefin tuna (*Thunnus thynnus*) larvae from the Gulf of Mexico and NW Mediterranean spawning grounds: A comparative stable isotope study. *PLoS ONE* (2015), 10, e0133406. [CrossRef]
54. Uriarte, A.; García, A.; Ortega, A.; De La Gándara, F.; Quintanilla, J.; Laiz-Carrión, R. Isotopic discrimination factors and nitrogen turnover rates in reared Atlantic bluefin tuna larvae (*Thunnus thynnus*): effects of maternal transmission. *Sci Mar* (2016), 80: 447-456. [CrossRef]
55. García, A.; Laiz-Carrión, R.; Uriarte, A.; Quintanilla, J.; Morote, E.; Rodriguez, J.; Alemany, F. Differentiated stable isotopes signatures between pre- and post-flexion larvae of Atlantic bluefin tuna (*Thunnus thynnus*) and of its associated tuna species of the Balearic Sea (NW Mediterranean). *Deep. Sea. Res*., Part II (2017), 140: 18-24. [CrossRef]
56. Starrs, D.; Davis, J.T.; Schlaefer, J.; Ebner, B.C.; Eggi ns, S.M.; Fulton, C.J. Maternally transmitted isotopes and their effects on larval fish: a validation of dual isotopic marks within a meta-analysis context. *Can. J. Fish. Aquat. Sci* (2014), 71, 387–397. [CrossRef]
57. Quintanilla, J. M.; Laiz-Carrión, R.; García, A.; Quintanilla, L. F.; Cortés, D.; Gómez-Jakobsen, F., et al. Early life trophodynamic influence on daily growth patterns of the Alboran Sea sardine (*Sardina pilchardus*) from two distinct nursery habitats (Bays of Málaga and Almería) in the Western Mediterranean Sea. *Mar. Env. Res* (2020), 162, 105195. [CrossRef]
58. Quezada-Romegialli, C.; Jackson, A. L.; Hayden, B.; Kahilainen, K. K.; Lopes, C.; Harrod, C. tRophic Position, an r package for the Bayesian estimation of trophic position from consumer stable isotope ratios. *Methods Ecol. Evol* (2018), 9, v1592–v1599. [CrossRef]
59. Polunin, N.V.C.; Pinnegar, J.K. Trophic ecology and the structure of marine food webs. In Handbook of Fish and Fisheries. Vol. I. Edited by P.J.B. Hart; J.C. Reynolds. Blackwell, *Oxford*, UK (2002), 310–320. [CrossRef]
60. Jackson, A. L.; Inger, R.; Parnell, A. C.; Bearhop, S. Comparing isotopic niche widths among and within communities: SIBER – Stable Isotope Bayesian Ellipses in R. *J. Anim. Ecol* (2011), 80, 595–602. [CrossRef]
61. Bearhop, S.; Adams, C.E.; Waldron, S.; Fuller, R.A.; MacLeod, H. Determining trophic niche width: a novel approach using stable isotope analysis. *J Anim Ecol* (2004), 73, 1007–1012. [CrossRef]
62. Newsome, S.; Martínez del Rio, C.; Bearhop, S.; Phillips, D. A niche for isotopic ecology. *Front. Ecol. Environ*. (2007), 5, 429–436. [CrossRef]
63. Syväranta, J.; Lensu, A.; Marjomäki, T.J.; Oksanen, S.; Jones, R.I. An empirical evaluation of the utility of convex hull and standard ellipse areas for assessing population niche widths from stable isotope data. *Plos One* (2013), 8(2), e56094. [CrossRef]
64. Gerard, T.; Lamkin, J.T; Kelly, B.T.; Knapp, N.A.; Laiz-Carrión, R.; Malca, E.; Selph, K.E.; Shiroza, A.; Shropshire, T.A.; Stukel, M.R; Swalethorp, R; Yingling, N.; Landry, MR. Bluefin Larvae in Oligotrophic Ocean Foodwebs, investigations of nutrients to zooplankton: overview of the BLOOFINZ-Gulf of Mexico program. *Journal of Plankton Research*, Volume 44, Issue 5, September/October (2022), Pages 600–617. [CrossRef]
65. Malca, E.; Quintanilla, J.M.; Gerard, T.; Alemany, F.; Sutton, T.; García, A.; Lamkin, J.T.; Laiz-Carrión, R. Differential larval growth strategies and trophodynamics of larval Atlantic bluefin tuna (*Thunnus thynnus*) from two discrete spawning grounds. *Front. Mar. Sci* (2023), 10, 1233249. [CrossRef]
66. Quintanilla, J.M.; Malca, E.; Gerard, T.; Lamkin, J.T.; García, A.; Laiz-Carrión, R. Evidence of isotopic maternal transmission for bluefin tuna (*Thunnus thynnus*) larval growth. *Mar. Env. Res* (2023), 190, 106112. [CrossRef]
67. Malca, E.; Shropshire, T. M.; Landry, M. R.; Quintanilla, J. M.; Laíz-Carrión, R.; Shiroza, A., et al. Influence of food quality on larval growth of Atlantic bluefin tuna (*Thunnus thynnus*) in the Gulf of Mexico. *J. Plankton Res* (2022), 44(5), 474–762. [CrossRef]
68. Logan, J.M.; Jardine, T.D.; Miller, T.J.; Bunn, S.E.; Cunjak, R.A.; Lutcavage, M.E. Lipid corrections in carbon and nitrogen stable isotope analyses: comparison of chemical extraction and modelling methods. *J Anim Ecol* (2008), 77, 838−846. [CrossRef]
69. Bode, A.; Alvarez-Ossorio, M.T.; Cunha, M.E.; Garrido, S.; Peleteiro, J.B.; Valdés, L., et al. Stable nitrogen isotope studies of the pelagic food web on the Atlantic Shelf of the Iberian Peninsula. *Prog. Oceanography* (2007), 74, 115-131. [CrossRef]
70. Varela, J. L.; de la Gándara, F.; Ortega, A.; Medina, A. 13C and 15N analysis in muscle and liver of wild and reared young-of-the-year (YOY) Atlantic bluefin tuna. *Aquac* (2012), 354-355, 17–21. [CrossRef]
71. Sokal, R.R.; Rohlf, F.J. Biometría. Principios y métodos estadísticos en la investigación biológica. Tursen, S.A. Hermann Blume Ediciones, Madrid. (1979)

72. Quintanilla, J.M.; Laiz-Carrión, R.; Uriarte, A.; García, A. Influence of trophic pathways on daily growth patterns of Western Mediterranean anchovy (*Engraulis encrasicolus*) larvae. *Mar. Ecol. Prog. Ser* (2015), 531, 263-275. [CrossRef]
73. Pepin, P.; Effect of temperature and size on development, mortality, and survival rates of the pelagic early life history stages of Marine Fish. *Can. J. Fish. Aquat. Sci* (1991), 48(3), 503-518. [CrossRef]
74. Chick, J.H.; Van Den Avyle, M.J. Effects of feeding ration on larval swimming speed and responsiveness to predator attacks: implications for cohort survival. *Can. J. Fish. Aquat. Sci* (2000), 57, 106–115. [CrossRef]
75. Pitchford, J.W.; Brindley, J. Prey patchiness, predator survival and fish recruitment. Bull. *Math. Biol* (2001), 63, 527–546. [CrossRef]
76. Hjort, J. Fluctuations in the great fisheries of Norther Europe. *Rapports et Procés-Verbaux* (1914), 20, 1-228. [CrossRef]
77. Hjort, J. Fluctuations in the year classes of important food fishes. *ICES Journal of Marine Science* (1926), 1(1), 5-38. [CrossRef]
78. Schismenou, E.; Giannoulaki, M.; Tsiaras, K.; Lefkaditou, E.; Triantafyllou, G.; Somarakis, S. Disentangling the effects of inherent otolith growth and model-simulated ecosystem parameters on the daily growth rate of Young anchovies. *Mar. Ecol. Prog. Ser* (2014), 515, 227–237. [CrossRef]
79. Takahashi, M.; Watanabe, Y. Growth rate-dependent recruitment of Japanese anchovy (Engraulis japonicus) in the Kuroshio–Oyashio transitional waters. *Mar. Ecol. Prog. Ser* (2004), 266, 227–238. [CrossRef]
80. Tsuda, Y.; Sakamoto, W.; Yamamoto, S.; Murata, O. Effect of environmental fluctuations on mortality of juvenile Pacific bluefin tuna, *Thunnus orientalis*, in closed life-cycle aquaculture. *Aquaculture* (2012), (330-333): 142-147. [CrossRef]
81. Aranda, G.; Abascal, F.J.; Varela, J.L.; Medina, A. Spawning Behaviour and Post-Spawning Migration Patterns of Atlantic Bluefin Tuna (*Thunnus thynnus*) Ascertained from Satellite Archival Tags. *Plos One* (2013). [CrossRef]
82. Varela, J.L.; Spares, A.D.; Stokesbury, M.J.W. Feeding ecology of Atlantic bluefin tuna (*Thunnus thynnus*) in the Gulf of Saint Lawrence, *Canada. Mar. Environ. Res*. (2020), 161, 105087. [CrossRef]
83. Goolish, E.M.; Alderman, I.R. Effects of ration size and temperature on the growth of juvenile common carp (*Cyprinus carpio L.). Aquaculture* (1984), (1-2), 27-35. [CrossRef]
84. Catalán, I.A.; Folkvord, A.; Palomera, I.; Quílez-Badía, G.; Kallianoti, F.; Tselepides, A.; Kallianotis, A. Growth and feeding patterns of European anchovy (*Engraulis encrasicolus*) early life stages in the Aegean Sea (NE Mediterranean). *Est.Coast.Shelf.Sci* (2010), 86, 299–312. [CrossRef]
85. Wilson, D.; Meekan, M.G. Growth-related advantages for survival to the point of replenishment in the coral reef fish *Stegastes partitus (Pomacentridae). Mar Ecol Prog Ser* (2002), 231, 247–260. [CrossRef]
86. Caldarone, E.M.; Onge-Burns, J.M.S.; Buckley, L.J. Relationship of RNA/DNA ratio and temperature to growth in larvae of Atlantic cod (*Gadus morhua*). *Mar Ecol Prog Ser* (2003), 262, 229–240. [CrossRef]
87. Kouwenberg, A.L.; Hipfner, J.M.; McKay, D.W.; Storey, A.E. Corticosterone and stable isotopes in feathers predict egg size in Atlantic Puffins Fratercula arctica. *Ibis* (2013), 155(2), 413–418. [CrossRef]
88. Bernardo, J.H. Maternal effects in animal ecology. *Am. Zool,* (1996). 36:83–105.
89. Letcher, B.H.; Rice, J.A.; Crowder, L.B.; Rose, K.A. Variability in survival of larval fish: disentangling components with a generalized individual-based model. *Can. J. Fish. Aquat. Sci* (1996), 53, 787-801. [CrossRef]
90. Sará, G.; Sará, R. Feeding habits and trophic levels of bluefin tuna (*Thunnus thynnus*) of different size classes in the Mediterranean Sea. *J. Appl. Ichthyol* (2007), 23, 122–127. [CrossRef]
91. Logan, J.M.; Rodríguez-Marín, E.; Goñi, N.; Barreiro, S.; Arrizabalaga, H.; Golet, W.; Lutcavage, M. Diet of young Atlantic bluefin tuna (Thunnus thynnus) in eastern and western Atlantic foraging grounds. Mar. Biol. (2011), 158, 73-85. [CrossRef]
92. Butler, C.M.; Logan, J.M.; Provaznik, J.M.; Hoffmayer, E.R.; Staudinger, M.D.; Quattro, J.M.; Roberts, M.A.; Ingram Jr., G.W.; Pollack, A.G.; Lutcavage, M.E. Atlantic bluefin tuna (*Thunnus thynnus*) feeding ecology in the northern Gulf of Mexico: a preliminary description of diet from the western Atlantic spawning grounds. *J. Fish Biol*. (2015), 86, 365–374. [CrossRef]
93. Sorell, J.M.; Varela, J.L.; Goñi, N.; Macías, D.; Arrizabalaga, H.; Madina, A. Diet and consumption rate of Atlantic bluefin tuna (*Thunnus thynnus*) in the Strait of Gibraltar. *Fis. Res*. (2017), 188, 112-120. [CrossRef]
94. Varela, J.L.; Rojo-Nieto, E.; Sorell, J.M.; Medina, A. Using stable isotope analysis to assess trophic relationships between Atlantic bluefin tuna (*Thunnus thynnus*) and striped dolphin (Stenella coeruleoalba) in the Strait of Gibraltar. *Mar. Environ. Res*. (2018), 139, 57-63. [CrossRef]
95. Lesser, J.S.; James, W.R.; Stallings, C.D.; Wilson, R.M.; Nelson, J.A. Trophic niche size and overlap decreases with increasing ecosystem productivity. *Oikos* (2020), 129(9), 1303-1313. [CrossRef]
96. Galuardi, B.; Royer, F.; Golet, W.; Logan, J.; Neilson, J.; Lutcavage, M. Complex migration routes of Atlantic bluefin tuna (*Thunnus thynnus*) question current population structure paradigm. *Can. J. Fish. Aquat. Sci* (2010), 67(6), 966–976. [CrossRef]

97. Wilson, S.G.; Lawson, G.L.; Stokesbury, M.J.W.; Spares, A.; Boustany, A.M.; Neilson, J.D.; Block, B.A. Movements of Atlantic bluefin tuna from the Gulf of St Lawrence to their spawning grounds. *ICCAT Col. Vol. Sci. Pap* (2011), 66(3), 1247–1256. [CrossRef]
98. MacArthur, R.H., Pianka, ER. On optimal use of a patchy environment. *Am. Nat*. (1996), 100, 603–609. [CrossRef]
99. O'Farrell, S., Bearhop, S., McGill, R.A.R., Dahlgren, C.P., Brumbaugh, D.R., Mumby, P.J. Habitat and body size effects on the isotopic niche space of invasive lionfish and endangered Nassau grouper. *Ecosphere* (2014), 5, 1–11. [CrossRef]
100. Montoya, J.P. Natural abundance of ^{15}N in marine planktonic ecosystems. In Stable Isotopes in Ecology and Environmental Science. Eds Michener, R. and Lajtha, K. Wiley-Blackwell, USA (2007), 176-194. [CrossRef]
101. Morote, E.; Olivar, M. P.; Pankhurst, P. M.; Villate, F and Uriarte, I. Trophic ecology of bullet tuna *Auxis rochei* larvae and ontogeny of feeding-related organs. *Mar. Ecol. Prog. Ser*. (2008), 353, 243-254. [CrossRef]
102. Kwan, G.T.; Walsh, K.A.; Thompson, A.R.; Ben-Aderet, N.J; Fennie H.W.; , Semmens B.X; Swalethorp, R. Trophic efficiency facilitates larval Shortbelly Rockfish (*Sebastes jordani*) development. *Mar. Coast. Fish*. Under review [CrossRef]
103. Caut, S.; Angulo, E.; Courchamp, F. (2009). Variation in discriminant factors ($\delta^{15}N$ and $\delta^{13}C$): the effect of diet isotopic values and applications for diet reconstruction. *J. Appl. Ecol*. (2009), 46, 443-453. [CrossRef]
104. Swalethorp, R.; Landry, M.R.; Semmens, B.X. et al. Anchovy boom and bust linked to trophic shifts in larval diet. *Nat Commun* (2023), 14, 7412. [CrossRef]
105. Stukel, M.R.; Gerard, T.; Kelly, T.B.; Knapp, A.N.; Laiz-Carrión, R.; Lamkin, J.T.; Landry, M. R.; Malca, E.; Selph, K.E.; Shiroza, A.; Swalethorp, R. Plankton food webs in the oligotrophic Gulf of Mexico spawning grounds of Atlantic bluefin tuna. J. Plankton Res. (2022), 44(5), 763–781. [CrossRef]
106. Landry, M.R.; Beckley, L.E.; Muhling, B.A. Climate sensitivities and uncertainties in food-web pathways supporting larval bluefin tuna in subtropical oligotrophic oceans. ICES Journal of Marine Science (2019), 76(2), 359–369. [CrossRef]
107. Knapp, A.N.; Thomas, R.K.; Stukel, M.R.; Kelly, T.B.; Landry, M.R.; Selph, K.E.; Malca, E.; Gerard, T.; Lamkin, John. Constraining the sources of nitrogen fueling export production in the Gulf of Mexico using nitrogen isotope budgets, *J. Plankton Res*. (2022), 44, 5, 692–710. [CrossRef]
108. Tilley, J. D.; Butler, C. M.; Suárez-Morales, E.; Franks, J. S.; Hoffmayer, E. R.; Gibson, D.; Comyns, B. H.; Ingram Jr, G. W.; et al. Feeding ecology of larval Atlantic bluefin tuna, *Thunnus thynnus,* from the central Gulf of Mexico. *Bull. Mar. Sci.* (2016), 92, 321–334. [CrossRef]
109. Uriarte A.; Johnstone, C.; Laiz-Carrión R.; García, A.; et. al. Evidence of density-dependent cannibalism in the diet of wild Atlantic bluefin tuna larvae *(Thunnus thynnus)* of the Balearic Sea (N.W. Mediterranean). *Fish. Res.* (2019), 212: 63-71. [CrossRef]
110. Landry, M.R.; Swalethorp, R. Mesozooplankton biomass, grazing and trophic structure in the bluefin tuna spawning area of the oceanic Gulf of Mexico. *J.Plankton.Res* (2022), 44, 5, 677–691. [CrossRef]
111. Wells, R.J.D.; Rooker, J.R. Feeding ecology of pelagic fish larvae and juveniles in slope waters of the Gulf of Mexico. *J. Fish. Bio* (2009), 75, 1719–1732. [CrossRef]
112. Kloppmann, M.H.F.; Hillgruber, N.; Von Westernhagen, H. Wind-mixing effects on feeding success and condition of blue whiting larvae in the Porcupine Bank area. *Mar. Ecol. Prog. Ser* (2002). 235: 263-277. [CrossRef]